Mass measurements in the vicinity of the rp-process and the νp-process paths with JYFLTRAP and SHIPTRAP

C. Weber[1],* V.-V. Elomaa[1],† R. Ferrer[2],‡ C. Fröhlich[3], D. Ackermann[4], J. Äystö[1], G. Audi[5], L. Batist[6], K. Blaum[2,4],§ M. Block[4], A. Chaudhuri[7],¶ M. Dworschak[4], S. Eliseev[4,6],§ T. Eronen[1], U. Hager[1],** J. Hakala[1], F. Herfurth[4], F.P. Heßberger[4], S. Hofmann[4], A. Jokinen[1], A. Kankainen[1], H.-J. Kluge[4,8], K. Langanke[4], A. Martín[4], G. Martínez-Pinedo[4], M. Mazzocco[4],†† I.D. Moore[1], J.B. Neumayr[9], Yu.N. Novikov[4,6], H. Penttilä[1], W.R. Plaß[4,10], A.V. Popov[6], S. Rahaman[1], T. Rauscher[11], C. Rauth[4], J. Rissanen[1], D. Rodríguez[12], A. Saastamoinen[1], C. Scheidenberger[4,10], L. Schweikhard[7], D.M. Seliverstov[6], T. Sonoda[1],‡‡ F.-K. Thielemann[11], P.G. Thirolf[9], and G.K. Vorobjev[4,6]

[1]*Department of Physics, University of Jyväskylä, FI-40014 Jyväskylä, Finland*
[2]*Institut für Physik, Johannes Gutenberg-Universität, D-55099 Mainz, Germany*
[3]*The Enrico Fermi Institute, Department of Astronomy and Astrophysics, The University of Chicago, Chicago, IL 60637, USA*
[4]*GSI-Darmstadt mbH, D-64291 Darmstadt, Germany*
[5]*CSNSM-IN2P3/CNRS, Université de Paris-Sud, F-91405 Orsay, France*
[6]*Petersburg Nuclear Physics Institute, 188300 Gatchina, St. Petersburg, Russia*
[7]*Institut für Physik, Ernst-Moritz-Arndt-Universität, D-17487 Greifswald, Germany*
[8]*Ruprecht-Karls-Universität Heidelberg, D-69120 Heidelberg, Germany*
[9]*Fakultät für Physik, Ludwig-Maximilians-Universität München, D-85748 Garching, Germany*
[10]*II. Physikalisches Institut, Justus-Liebig-Universität, D-35392 Gießen, Germany*
[11]*Departement für Physik, Universität Basel, CH-4056 Basel, Switzerland and*
[12]*Universidad de Huelva, Avda. de las Fuerzas Armadas s/n, E-21071 Huelva, Spain*

(Dated: August 29, 2008)

The masses of very neutron-deficient nuclides close to the astrophysical rp- and νp-process paths have been determined with the Penning trap facilities JYFLTRAP at JYFL/Jyväskylä and SHIPTRAP at GSI/Darmstadt. Isotopes from yttrium ($Z = 39$) to palladium ($Z = 46$) have been produced in heavy-ion fusion-evaporation reactions. In total 21 nuclides were studied and almost half of the mass values were experimentally determined for the first time: ^{88}Tc, $^{90-92}$Ru, $^{92-94}$Rh, and ^{94,95}Pd. For the ^{95}Pd^m, $(21/2^+)$ high-spin state, a first direct mass determination was performed. Relative mass uncertainties of typically $\delta m/m = 5\times10^{-8}$ were obtained. The impact of the new mass values has been studied in νp-process nucleosynthesis calculations. The resulting reaction flow and the final abundances are compared to those obtained with the data of the Atomic Mass Evaluation 2003.

PACS numbers: 07.75.+h Mass spectrometers, 21.10.Dr Binding energies and masses, 26.30.-k Nucleosynthesis in novae, supernovae, and other explosive environments, 26.50.+x Nuclear physics aspects of novae, supernovae, and other explosive environments
Keywords: atomic mass, nucleosynthesis, νp-process, reaction rates, ^{84}Y, ^{87}Zr, ^{88}Mo, ^{89}Mo, ^{88}Tc, ^{89}Tc, ^{90}Tc, ^{91}Tc, ^{92}Tc, ^{90}Ru, ^{91}Ru, ^{92}Ru, ^{93}Ru, ^{94}Ru, ^{92}Rh, ^{93}Rh, ^{94}Rh, ^{95}Rh, ^{94}Pd, ^{95}Pd, ^{95}Pd^m, ^{96}Pd determined with the Penning trap mass spectrometers JYFLTRAP and SHIPTRAP

I. INTRODUCTION

Direct mass measurements of exotic nuclei have advanced considerably due to the introduction of Penning-trap-based approaches at on-line facilities [1, 2, 3]. At present, relative uncertainties on the order of 5×10^{-8} or better are routinely achieved. These results provide important contributions towards studies of nuclear structure evolution far from stability. In particular, the high accuracy can play a crucial role in investigations of nuclei near the $N = Z$ line in the form of precision tests of the weak interaction [4, 5, 6], charge-symmetry effects in nuclear structure [7], and in nuclear astrophysics [8, 9].

In this paper we report on accurate mass measurements of neutron-deficient yttrium to palladium isotopes to ascertain their impact on the nucleosynthesis of

*Electronic address: christine.weber@phys.jyu.fi
†This publication comprises part of the Ph.D. thesis of V.-V. Elomaa.
‡This publication comprises part of the Ph.D. thesis of R. Ferrer.; Present address: NSCL, Michigan State University, East Lansing, MI 48824-1321, USA.
§Present address: Max-Planck-Institut für Kernphysik, D-69117 Heidelberg, Germany.
¶Present address: Department of Physics and Astronomy, University of Manitoba, Winnipeg, MB, R3T2N2, Canada.
**Present address: TRIUMF, 4004 Wesbrook Mall, Vancouver BC, V6T 2A3, Canada.
††Present address: Dipartimento di Fisica and INFN - Sezione di Padova, via Marzolo 8, I-35131 Padova, Italy.
‡‡Present address: Atomic Physics Laboratory, RIKEN, 2-1 Hirosawa, Wako, Saitama 351-0198, Japan.

neutron-deficient isotopes below tin. In this region, the rapid proton-capture process (rp-process) runs along the $N = Z$ line as a sequence of (p,γ) reactions followed by β^+ decays. This process is associated with accreting neutron stars where explosive hydrogen burning gives rise to the observed X-ray bursts. For very exotic nuclides close to the proton drip line, direct reaction-rate measurements are hampered by low production cross sections. Consequently, the necessary reaction rates have to be evaluated by theoretical models where the nuclear masses are one of the key input quantities. For low enough temperatures the rates are determined by individual resonances and depend exponentially on the resonance energy [10]. For higher temperatures many resonances are located in the Gamow window and therefore statistical models are applicable.

While the rp-process is necessary to explain the observed X-ray bursts, its contribution to the solar abundances is doubtful as the produced nuclei are not ejected from the neutron star. In the same mass region the νp-process [11, 12, 13] occurs as sequence of (p,γ) and (n,p) or β^+ reactions producing neutron-deficient nuclei with $A > 64$. This process occurs in proton-rich supernova ejecta under the influence of strong neutrino and antineutrino fluxes which produce neutrons via antineutrino absorption on free protons. The (n,p) reactions allow to overcome the long β-decay half-lives. After the temperature drops, proton-capture reactions freeze out and matter decays back to the line of β stability. In this way, neutron-deficient nuclei are produced and ejected in the supernova explosion.

II. EXPERIMENTAL SETUP AND PROCEDURE

The data presented in this paper were obtained within joint experiments at two facilities: SHIPTRAP at GSI and JYFLTRAP in Jyväskylä. Although the stopping and separation mechanisms for short-lived, exotic species are different at each facility, the basic functional units of the Penning trap setups are identical. Figure 1 shows the schematic layout for both Penning trap mass spectrometers, indicating their differences and similarities.

The IGISOL facility provides nuclides after bombarding a thin target with a beam from the Jyväskylä K-130 cyclotron. The reaction products recoil into helium gas at pressures of typically $p \approx 200$ mbar and thermalize therein, ending with a high fraction as singly-charged ions [14]. After extraction by the helium flow and electric field guidance, the ions pass through a dipole magnet at an energy of $30 - 40$ keV, where they are mass-separated with a resolving power of up to $R = 500$ and finally delivered to the JYFLTRAP system. One of the main advantages of this chemically non-selective method is the availability of refractory elements.

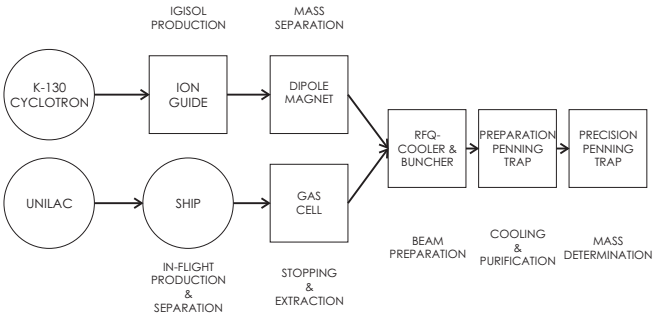

FIG. 1: Functional layout of the Penning trap mass spectrometers JYFLTRAP/JYFL (top) and SHIPTRAP/GSI (bottom). For a detailed description see text.

The SHIPTRAP facility [15, 16] is located behind the velocity filter SHIP [17, 18] at GSI/Darmstadt. Here, short-lived nuclides are produced by fusion-evaporation reactions in a thin target and are separated from the primary beam in a double Wien filter. The major physics goals of this experimental setup are the studies of transuranium elements, which cannot be accessed at other trap facilities. The reaction products from SHIP with energies of a few 100 keV/u are stopped in a buffer-gas filled stopping cell [19]. The ions are extracted from the gas cell by a combination of DC- and RF-electric fields through a nozzle. Subsequently, they are pre-cooled in an extraction radiofrequency quadrupole (RFQ) operated as an ion guide.

In both experiments, exotic ion beams are produced, decelerated, cooled and purified prior to their mass determination in the Penning trap. The extracted ion beam enters a gas-filled radiofrequency quadrupole (RFQ) cooler and buncher [20, 21] where the continuous beam is cooled and bunched for an efficient injection into the respective Penning trap system. These are nearly identical and have been developed in a common effort [22, 23, 24]. Both traps are open-endcap, cylindrical Penning traps [25], with a 7-electrode electrode configuration [26] for the preparation trap. The second trap, for the mass determination, is of identical geometry as the first one at JYFLTRAP, whereas at SHIPTRAP a 5-electrode trap with a reduced storage region is employed. They are placed in the warm bore of the same type of superconducting solenoid with two homogeneous centers at a field strength of $B = 7$ T. The relative inhomogeneities of the magnetic fields $\Delta B/B$ within 1 cm^3 are close to 1 ppm and 0.1 ppm at the positions of the first and the second trap, respectively.

In the first Penning trap a mass-selective buffer-gas cooling scheme [27] is employed in order to separate individual nuclides. The resolving power, $R = \nu_c/\Delta\nu_{c,\mathrm{FWHM}} = m/\Delta m$, that can be obtained in this process reaches up to $R \approx 1 \times 10^5$. In this way, individual isobars, or for some cases even isomers, can be selected. In the second Penning trap the mass m of a stored ion species with charge q is determined via a

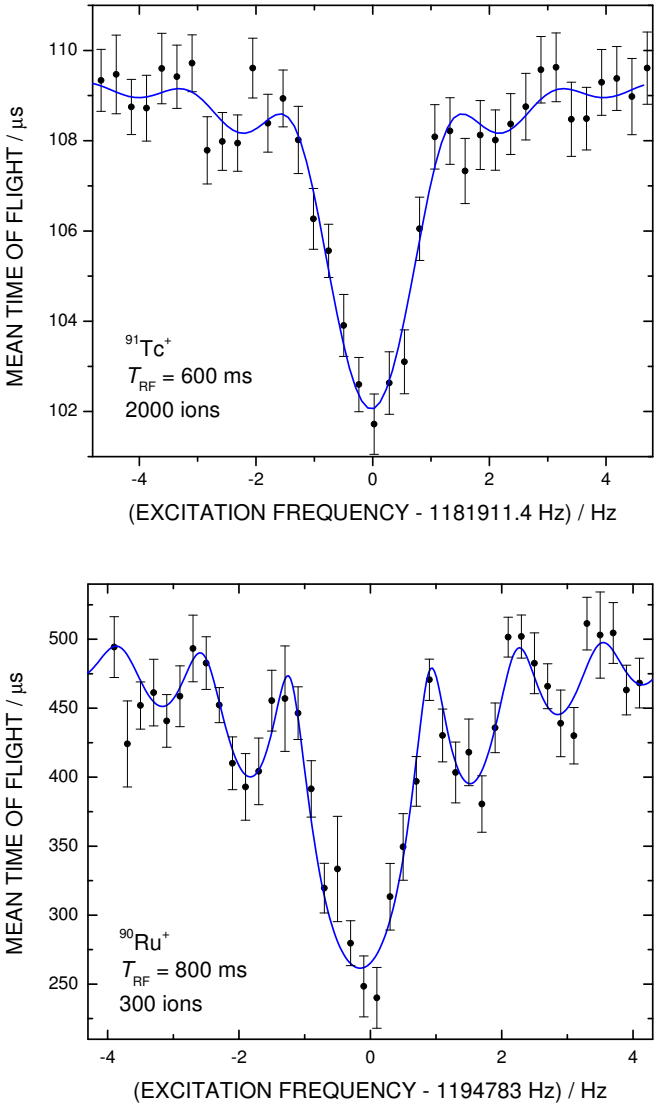

FIG. 2: Cyclotron resonance curves for $^{91}Tc^{+}$ ions (top) measured at SHIPTRAP and $^{90}Ru^{+}$ ions (bottom) measured at JYFLTRAP. The duration of the RF excitation T_{RF} and the number of detected ions are given.

measurement of its cyclotron frequency $\nu_c = qB/(2\pi m)$. A cyclotron resonance curve is obtained by the time-of-flight detection method: an increase in radial kinetic energy resulting from the resonant excitation of both radial ion motions with an RF-field at ν_c is detected by a reduction in the time of flight of the ejected ions towards a detector [28, 29]. Figure 2 shows examples of cyclotron resonance curves for singly-charged ^{91}Tc and ^{90}Ru ions from the SHIPTRAP and JYFLTRAP experiments, respectively.

Figure 3 displays a section of the nuclear chart below the doubly-magic shell closure of ^{100}Sn. The nuclides studied at the SHIPTRAP (dark grey) and JYFLTRAP (light grey) facilities are approaching the $N = Z$ line. A possible pathway of the rp-process for steady-state burning (from Schatz [30], solid lines) is shown together with a possible path of the νp-process (this work, dashed lines). In Table I, half-lives $T_{1/2}$, spin-parities I^{π}, and excitation energies of the first isomeric states E_{ex} are listed for the studied nuclides according to the latest NUBASE compilation [37]. In the calculation of reaction networks for astrophysical purposes, a preceding unambiguous mass-to-state assignment is essential. This overview helps to judge if the presence of a particular state can be excluded right away during our measurement process: states with a half-life $T_{1/2} \leq 10$ ms will not reach the setup. On the other hand, a separation of isomers will not be feasible if the excitation energy E_{ex} of the specific ion is smaller than the mass resolution [128]; for example, $E_{ex} \approx 75$ keV was employed for ^{88}Tc. The mass-to-state assignment in this work is based on the present knowledge on these nuclides and is discussed in Sec. V.

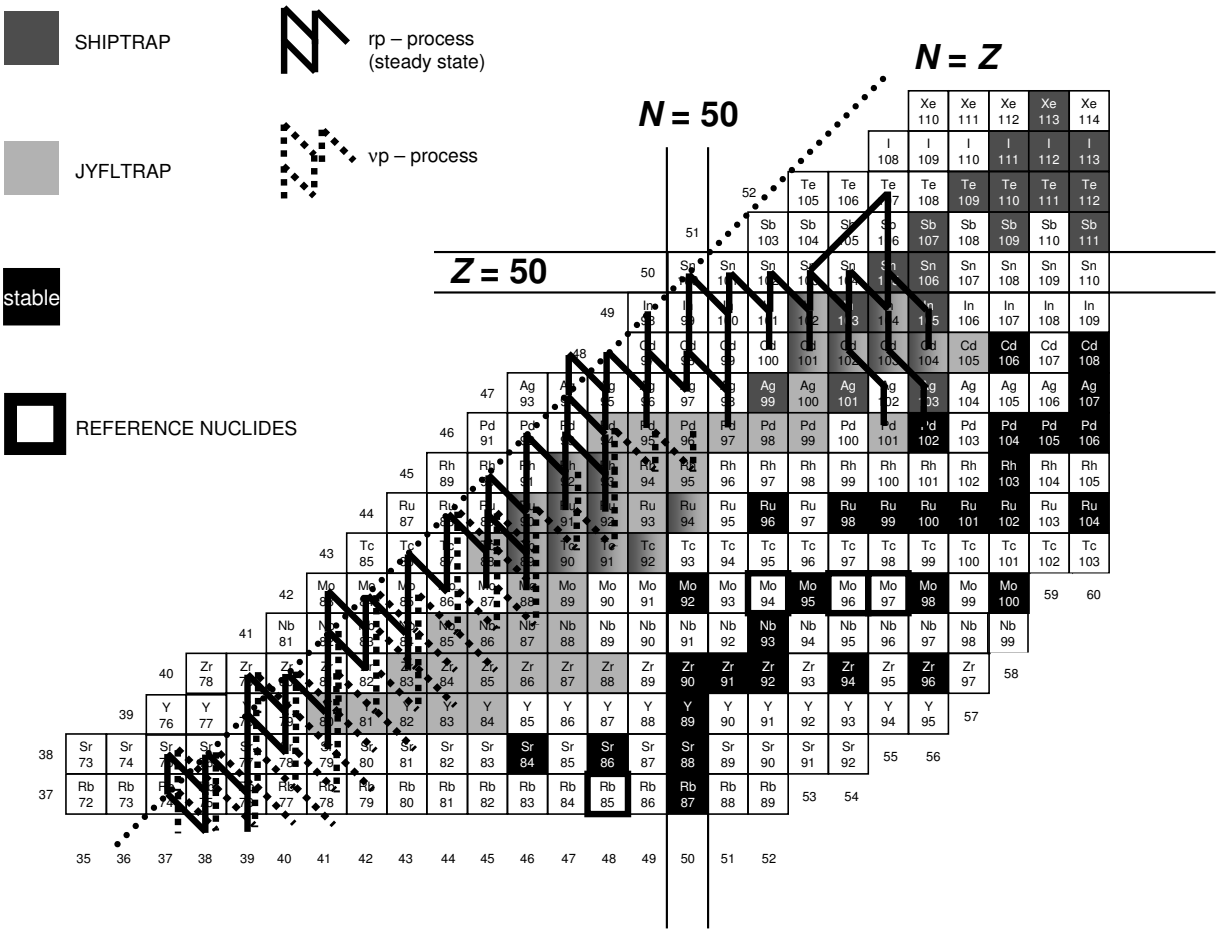

FIG. 3: Nuclides studied at JYFLTRAP (light grey) and SHIPTRAP (dark grey). The present paper reports on masses of ^{84}Y, ^{87}Zr and isotopes of molybdenum, technetium, ruthenium, rhodium, and $^{94-96}$Pd. All other nuclides measured by either trap facility are published in Refs. [31, 32, 33]. The $N = Z$ line was reached in measurements with the mass spectrometer ISOLTRAP for rubidium [34, 35] and strontium isotopes [35, 36].

TABLE I: Properties of the nuclides investigated in this work with half-life $T_{1/2}$, spin-parity I^π, and excitation energy of the first isomeric states $E_{\rm ex}$ from Ref. [37]. '*' denotes nuclides where the uncertainty of the excitation energy $E_{\rm ex}$ is larger than half of the energy ($\sigma \geq E_{\rm ex}/2$) and '&' those cases where the ordering of the ground and isomeric states have been reversed compared to the Evaluated Nuclear Structure Data File (ENSDF) [38]. The parenthesis in the third column indicates uncertain values of spin and/or parity, while '#' indicates a value that is estimated from systematic trends from neighboring nuclides with the same Z and N parities.

Nuclide		Half-Life $T_{1/2}$		Spin/Parity I^π	Excitation energy $E_{\rm ex}$ / keV
^{84}Y	*	4.6	s	1^+	
^{84}Y^m	*	39.5	min	(5^-)	-80(190)
^{87}Zr		1.68	h	$(9/2)^+$	
^{87}Zr^m		14.0	s	$(1/2)^-$	335.84(19)
^{88}Mo		8.0	min	0^+	
^{89}Mo		2.11	min	$(9/2^+)$	
^{89}Mo^m		190	ms	$(1/2^-)$	387.5(2)
^{88}Tc	*	5.8	s	(2,3)	
^{88}Tc^m	*	6.4	s	(6,7,8)	0(300)#
^{89}Tc		12.8	s	$(9/2^+)$	
^{89}Tc^m		12.9	s	$(1/2^-)$	62.6(5)
^{90}Tc	*&	8.7	s	1^+	
^{90}Tc^m	*&	49.2	s	(8^+)	310(390)
^{91}Tc		3.14	min	$(9/2)^+$	
^{91}Tc^m		3.3	min	$(1/2)^-$	139.3(3)
^{92}Tc		4.25	min	$(8)^+$	
^{92}Tc^m		1.03	μs	(4^+)	270.15(11)
^{90}Ru		11	s	0^+	
^{91}Ru	*	9	s	$(9/2^+)$	
^{91}Ru^m	*	7.6	s	$(1/2^-)$	80(300)#
^{92}Ru		3.65	min	0^+	
^{93}Ru		59.7	s	$(9/2)^+$	
^{93}Ru^m		10.8	s	$(1/2)^-$	734.4(1)
^{93}Ru^n		2.20	μs	$(21/2)^+$	2082.6(9)
^{94}Ru		51.8	min	0^+	
^{94}Ru^m		71	μs	(8^+)	2644.55(25)
^{92}Rh		4.3	s	$(6^+)^a$	
^{93}Rh		13.9	s	$9/2^+$#	
^{94}Rh	*	70.6	s	$(2^+, 4^+)$	
^{94}Rh^m	*	25.8	s	(8^+)	300(200)#
^{95}Rh		5.02	min	$(9/2)^+$	
^{95}Rh^m		1.96	min	$(1/2)^-$	543.3(3)
^{94}Pd		9.0	s	0^+	
^{94}Pd^m		530	ns	(14^+)	4884.4(5)
^{95}Pd		10#	s	$9/2^+$#	
^{95}Pd^m		13.3	s	$(21/2^+)$	1860(500)#^{b}
^{96}Pd		122	s	0^+	
^{96}Pd^m		1.81	μs	8^+	2530.8(1)

[a] A low-spin isomeric state with $T_{1/2} = 0.53$ s has been observed in Ref. [39].

[b] An excitation energy of about 2 MeV was obtained in Ref. [40].

III. DATA ANALYSIS

The results of our mass measurements are given as frequency ratios, $r = \nu_{\mathrm{c,ref}}/\nu_{\mathrm{c}}$, between the cyclotron frequencies of a reference ion and the ion of interest. This ratio can be written as

$$r = \frac{\nu_{\mathrm{c,ref}}}{\nu_c} = \frac{z_{\mathrm{ref}}}{z} \cdot \frac{m - (z \cdot m_e)}{m_{\mathrm{ref}} - (z_{\mathrm{ref}} \cdot m_e)} \; . \qquad (1)$$

In order to determine the mass m from this expression one has to consider the inevitable drift of the magnetic field strength B, which has to be known at the moment when the ion of interest was studied. To this end, the measurement of a reference ion with well-known mass, before and after the measurement of the ion of interest, is used to determine the actual value of B. In the case of singly-charged ions $z = z_{\mathrm{ref}} = 1$ the mass value is calculated by

$$m = r(m_{\mathrm{ref}} - m_e) + m_e \, , \qquad (2)$$

where m_e is the electron mass. The physics of a stored ion in a Penning trap including its motion as well as influences from field imperfections are extensively described in Refs. [41, 42, 43, 44, 45]. Contributions to the total uncertainty in a frequency determination were quantified in systematic experimental studies at the ISOLTRAP mass spectrometer [46, 47] and the analysis of the data presented here was followed accordingly. In the following, a concise description of the contributions to the total uncertainty is given.

1. A least-squares fit of the theoretical line shape [29] to the experimental data points was initially performed. From this fit the cyclotron frequency ν_c and its statistical uncertainty σ_s were obtained. The latter is inversely proportional to the number of detected ions, *i.e.* $\sigma_s \propto 1/\sqrt{N_{\mathrm{ions}}}$.

2. A count-rate class analysis [47] was performed to correct possible frequency shifts from influences of contaminants, as, for example, other isobars or isomeric states. In some cases such an analysis was not feasible due to insufficient statistics. Here, the uncertainty of the cyclotron resonance frequency was increased according to a comparison between results without and with count-rate class analysis in high-statistics measurements of other short-lived nuclides. This accounts for the larger uncertainty after such an analysis, in order not to even favor those measurements with particularly low statistics.

3. A pair of measurements of the reference ion, before and after the measurement of the investigated radioactive ion, is performed to calibrate the magnetic field B. A linear interpolation is used to calculate the value of B at the time of the measurement of the radioactive ion of interest. With these data a frequency ratio $r = \nu_{\mathrm{c,ref}}/\nu_{\mathrm{c}}$ was calculated. Fluctuations of the magnetic field strength in addition to the linear trend are assumed to be of statistical nature. The longer the duration between reference measurements, the larger the spread of such fluctuations. Therefore this time-dependent uncertainty is quadratically added to the uncertainty of each frequency ratio. Their magnitudes were determined in long-term frequency measurements of ions, $^{133}Cs^{+}$ and $^{85}Rb^{+}$ for SHIPTRAP [48], and $^{54}Fe^{+}$ for JYFLTRAP [49]. Accordingly, the time-dependent quantities of $\sigma_B(\nu_{\mathrm{ref}})/\nu_{\mathrm{ref}} = 4.4 \cdot 10^{-9}\,\mathrm{h}^{-1} \cdot \Delta t$ and $\sigma_B(\nu_{\mathrm{ref}})/\nu_{\mathrm{ref}} = 1.9 \cdot 10^{-9}\,\mathrm{h}^{-1} \cdot \Delta t$ have been used in these data, respectively.

4. The weighted mean of the available frequency ratios for a given nuclide was calculated and the consistency of internal versus external uncertainties was compared [50]. The ratios of both were found to be very close to unity in all cases for both sets of data indicating that only statistical fluctuations due to random deviations are present in the experimental data. The larger value of the two was taken as the final uncertainty. In this way the uncertainties are always given conservatively.

5. By means of cross-reference mass measurements with carbon clusters [51], which provide absolute frequency ratios, a relative mass-dependent shift of $\sigma_m(r)/r = (1.1 \pm 1.7) \cdot 10^{-10}/u \cdot \Delta m$ was obtained at SHIPTRAP, where Δm indicates the difference in mass between the radionuclide of interest and the reference ion $(m - m_{\mathrm{ref}})$. At the JYFLTRAP facility this quantity has been determined via a mass comparison of oxygen $^{16}O_2^{+}$ to xenon $^{132}Xe^{+}$ ions to be $|\sigma_m(r)/r| = 7 \cdot 10^{-10}/u \cdot \Delta m$. For the SHIPTRAP data, the averaged frequency ratios were corrected by this mass-dependent frequency shift and the same quantity was quadratically added to its uncertainty, whereas for JYFLTRAP no correction was applied due to the undetermined sign of this quantity. Since the accurate frequency ratios of carbon clusters of different sizes are known without any uncertainty [129] the relative residual uncertainty was determined to be $\sigma_{\mathrm{res}}(r)/r = 4.5 \cdot 10^{-8}$ with carbon clusters at SHIPTRAP [51]. Since this quantity has not yet been experimentally determined at JYFLTRAP, the deviation between previous JYFLTRAP data and precise experimental AME2003 values in this mass region have been compared. Their relative average deviation is about $5 \cdot 10^{-8}$. The residual uncertainty and the latter estimate have been added to give the final uncertainty of the frequency ratio in either experiment.

IV. RESULTS

The data reported here were obtained during several on-line runs at the SHIPTRAP/GSI and JYFLTRAP/IGISOL facilities. The measurements at SHIPTRAP were performed in July 2006 [53]. In that work, the UNILAC primary beam of ^{40}Ca ions at 200 MeV energy was used in combination with a 0.5 mg/cm^2 target of ^{58}Ni (enriched to 99.9%) in order to produce neutron-deficient species of technetium, ruthenium, and rhodium in the region around $A = 90$ via fusion-evaporation reactions. The identical reaction was used in August 2006 at JYFLTRAP [54], where a $^{\rm nat}$Ni target [130] of 3.6 mg/cm^2 foil thickness was used in combination with a beam of 189 MeV (JYFLTRAP II) or 220 MeV (JYFLTRAP III) ^{40}Ca ions. In addition, a beam of ^{36}Ar at 222 MeV (JYFLTRAP I) energy was employed to produce ^{84}Y, ^{87}Zr, ^{89}Mo, and ^{88}Tc ions. In a second experiment with JYFLTRAP in December 2006 a ^{40}Ca beam at 205 MeV (JYFLTRAP IV) and 170 MeV energy (JYFLTRAP V) was used to produce the $A = 91$ isobars of technetium and ruthenium and the isotopes of palladium, respectively.

All results from the cyclotron frequency determination at JYFLTRAP and SHIPTRAP are presented in Table II. In the second column the experiment is indicated to refer to the parameters for the production of these exotic nuclides as given above. The third column lists the number of detected ions in all cyclotron resonance curves and in column four and five the reference nuclide and the resulting frequency ratios $r = \nu_{\rm c,ref}/\nu_{\rm c}$ are given. For ten nuclides the cyclotron frequencies have been determined at both experiments, SHIPTRAP and JYFLTRAP. In these cases, a weighted mean of the frequency ratio is given. From the experimental results the mass excess of the nuclide under study is derived using the atomic masses of ^{97}Mo, ^{16}O, ^{85}Rb, or ^{94}Mo from the Atomic Mass Evaluation, AME2003 [55]. The final values are compared with those from AME2003 and their differences are given in the last column.

A graphical representation of the mass differences between AME2003 and this work is shown in Fig. 4. For the ten nuclides studied by both experiments, the Penning trap results agree in all cases perfectly with each other. They yield final weighted averages, which, along with the individual JYFLTRAP data, are set to zero in the diagram. The literature values are indicated by open symbols, whereas the positions of excited isomeric nuclear states are depicted as triangles. Within each of the individual isotopes an increasing deviation is visible departing from the valley of stability. This might be partly explained due to literature values having been extrapolated from systematic trends (see Table II). Note that for ^{95}Pd the mass values of the ground as well as of the $(21/2^+)$ isomeric state were determined.

TABLE II: Results from cyclotron frequency determinations at SHIPTRAP and JYFLTRAP. The experimental parameters for the production of these nuclides are given in the text. The cyclotron frequency ratio r to a singly-charged reference ion 'Ref' is given in the fifth column. The data from both experiments are averaged for the frequency ratios r or the deduced mass excess values ME. The latter were derived using the atomic masses of ^{97}Mo, ^{16}O, ^{85}Rb, or ^{94}Mo from the Atomic Mass Evaluation 2003 [55]. The final values are compared with those from AME2003 and their differences Δ are given in the last column. '#' indicates a value that is estimated from systematic experimental trends.

Nuclide	Experiment	N_{ions}	Ref	Frequency ratio r	ME_{TRAP} / keV	ME_{AME2003} / keV	$\Delta_{\mathrm{AME2003\text{-}TRAP}}$ / keV
^{84}Y	JYFLTRAP I	1918	^{97}Mo	1.031056762(53)[a]	-73922(19)[b]	-74160(90)	-238(92)
^{87}Zr	JYFLTRAP I	3673	^{97}Mo	1.061954361(54)[c]	-79341.4(5.3)	-79348(8)	-7(10)
^{88}Mo	JYFLTRAP II	8576	^{85}Rb	1.035450878(48)	-72686.5(3.8)	-72700(20)	-14(20)
^{89}Mo	JYFLTRAP I	2871	^{85}Rb	1.047198443(49)	-75015.0(3.9)	-75004(15)	11(15)
^{88}Tc	JYFLTRAP I	8715	^{85}Rb	1.035590047(48)	-61679(87)[d]	-62710(200)#	-1031(218)#
^{89}Tc	JYFLTRAP III	9817	^{85}Rb	1.047294785(48)			
^{89}Tc	SHIPTRAP	879	^{85}Rb	1.047294809(203)			
^{89}Tc	AVERAGE		^{85}Rb	1.047294786(47)	-67394.8(3.7)	-67840(200)#	-445(200)#
^{90}Tc	JYFLTRAP III	8503	^{85}Rb	1.059029703(49)			
^{90}Tc	SHIPTRAP	2516	^{85}Rb	1.059029697(94)			
^{90}Tc	AVERAGE		^{85}Rb	1.059029702(43)	-70723.7(3.4)	-71210(240)	-486(240)
^{91}Tc	JYFLTRAP IV	2291	^{94}Mo	0.968194724(47)	-75983.4(4.5)		
^{91}Tc	SHIPTRAP	5890	^{85}Rb	1.070740167(63)	-75986.5(5.0)		
^{91}Tc	AVERAGE				-75984.8(3.3)	-75980(200)	5(200)
^{92}Tc	JYFLTRAP II	9399	^{85}Rb	1.082480001(50)			
^{92}Tc	SHIPTRAP	7638	^{85}Rb	1.082480188(137)			
^{92}Tc	AVERAGE		^{85}Rb	1.082480023(47)	-78924.7(3.7)	-78935(26)	-10(26)
^{90}Ru	JYFLTRAP III	823	^{85}Rb	1.059103508(55)			
^{90}Ru	SHIPTRAP	259	^{85}Rb	1.059103727(127)			
^{90}Ru	AVERAGE		^{85}Rb	1.059103543(50)	-64883.3(4.0)	-65310(300)#	-427(300)#
^{91}Ru	JYFLTRAP II	7279	^{85}Rb	1.070838119(49)	-68239.1(3.9)		
^{91}Ru	JYFLTRAP IV	1510	^{94}Mo	0.968283302(50)	-68235.3(4.7)		
^{91}Ru	SHIPTRAP	1111	^{85}Rb	1.070838208(131)	-68232.0(10.4)		
^{91}Ru	AVERAGE				-68237.1(2.9)	-68660(580)#	-423(580)#
^{92}Ru	JYFLTRAP III	3744	^{85}Rb	1.082538479(51)			
^{92}Ru	SHIPTRAP	5691	^{85}Rb	1.082538554(67)			
^{92}Ru	AVERAGE		^{85}Rb	1.082538507(41)	-74299.0(3.2)	-74410(300)#	-111(300)#
^{93}Ru	JYFLTRAP III	5748	^{85}Rb	1.094278655(51)	-77214.0(4.0)	-77270(90)	-56(90)
^{94}Ru	JYFLTRAP II	5589	^{85}Rb	1.105987814(53)			
^{94}Ru	SHIPTRAP	1093	^{85}Rb	1.105987624(289)			
^{94}Ru	AVERAGE		^{85}Rb	1.105987808(52)	-82580.6(4.1)	-82568(13)	13(14)
^{92}Rh	JYFLTRAP III	1804	^{85}Rb	1.082681373(55)			
^{92}Rh	SHIPTRAP	220	^{85}Rb	1.082681725(434)			
^{92}Rh	AVERAGE		^{85}Rb	1.082681379(55)	-62999(15)[e]	-63360(400)#	-361(400)#
^{93}Rh	JYFLTRAP III	1437	^{85}Rb	1.094382341(53)			
^{93}Rh	SHIPTRAP	1035	^{85}Rb	1.094382514(141)			
^{93}Rh	AVERAGE		^{85}Rb	1.094382362(50)	-69011.3(3.9)	-69170(400)#	-159(400)#
^{94}Rh	JYFLTRAP II,III	1515	^{85}Rb	1.106110107(54)	-72907.5(4.2)	-72940(450)#	-33(450)#
^{95}Rh	JYFLTRAP II	1965	^{85}Rb	1.117818397(53)	-78342.3(4.2)	-78340(150)	2(150)
^{94}Pd	JYFLTRAP V	1606	^{94}Mo	1.000255075(49)	-66097.9(4.7)	-66350(400)#	-252(400)#
^{95}Pd	JYFLTRAP V	1470	^{94}Mo	1.010860017(50)	-69961.6(4.8)	-70150(400)#	-188(400)#
^{95}Pd^{m}	JYFLTRAP V	5307	^{94}Mo	1.010881456(48)	-68086.2(4.7)	-68290(300)	-204(300)
^{96}Pd	JYFLTRAP V	3570	^{94}Mo	1.021438050(48)	-76179.0(4.7)	-76230(150)	-51(150)

[a] This ratio was measured for YO^+ ions.

[b] The original value of −73888.8(5.2) keV was modified for an unknown mixture of isomeric states.

[c] This ratio was measured for ZrO^+ ions.

[d] The original error of 3.8 keV was increased due to the unknown level scheme of isomeric states.

[e] The original error of 4.3 keV was increased due to the unknown level scheme of isomeric states.

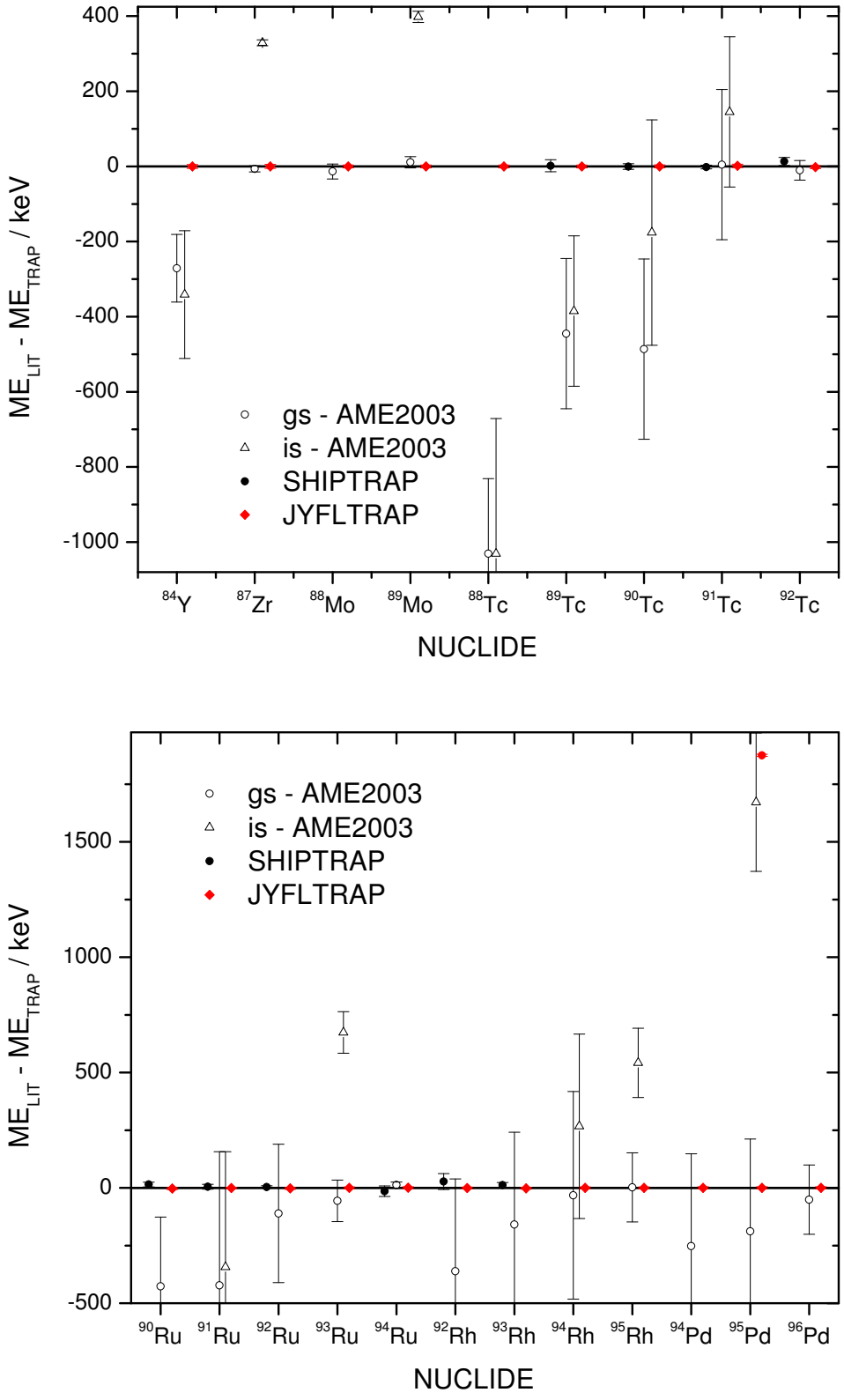

FIG. 4: Differences between experimental mass excess values from SHIPTRAP and JYFLTRAP with respect to the literature (AME2003) [37, 55]. When data from both trap experiments are available, the weighted average is taken as the final result ME_{TRAP} and set to zero. Open triangles indicate the position of the first excited isomeric state with respect to the AME2003 ground-state mass value. Color figure online.

V. DISCUSSION

In this discussion, some of the nuclides are grouped such as odd-even and even-odd ones with assigned spin values of $9/2^+$ and $1/2^-$, or nuclides where additional isomeric states are excluded due to their short half-lives. The remaining cases are discussed with increasing Z and A. It should be noted that seven of the nuclides investigated in this work ($^{90-92}$Tc, ^{93,94}Ru, and ^{94,95}Rh), were already studied with the Canadian Penning Trap (CPT) at the Argonne National Laboratory [56]. Since these data are published only in the form of a diagram, a quantitative comparison is omitted here. However, a qualitative comparison indicates similar mass values, obtained in both experiments following a production with heavy-ion fusion-evaporation reactions.

^{84}Y: This nucleus has a 39.5-min isomer with different assignments of spin values $I^\pi = 4^-$ [57], 5^- [58, 59], or 6^+ [60] and a $I^\pi = 1^+$ low-spin state with a half-life of 4.6 s. The level scheme has been under continuous debate with claims that the ground state is most likely the 39.5-min state [57] as well as the shorter-lived 1^+ state [59]. The Q_{EC} values of both β-decaying isomers [58] place the 5^- state energetically lower than the 1^+ state although with a very high uncertainty. Hence, their reversed placement according to the systematics in AME2003 results in a negative value of the excitation energy in Table I. The most recent experiment, in-beam studies carried out at NBI (Copenhagen) and Florida State University, propose a 40-min, 6^+ ground state and a 1^+ isomer at an excitation energy of 67 keV [60].
However, the mass resolution employed in our study of around 100 keV for the measured YO^+ ion is not sufficient to resolve ground and isomeric states and no count-rate class analysis has been carried out due to low statistics. Therefore, a correction according to a treatment for an unknown mixture of isomers [61] has been applied, modifying the original mass excess value from $-73888.8(5.2)$ keV to $-73922(19)$ keV.

^{88}Mo: The mass excess value determined at JYFLTRAP agrees with the value of the AME2003, which is deduced from the measured Q value of the ^{92}Mo(α,^{8}He)^{88}Mo reaction studied at INS, Tokyo [62], having a precision of 20 keV.

^{90}Tc: Prior to the Penning trap measurements, the radioactive nuclide ^{90}Tc was produced by a (p,3n) reaction on isotopically enriched ^{92}Mo at 43 MeV beam energy and studied by means of β-decay spectroscopy in two independent experiments at Foster Radiation Laboratory in Canada [63, 64]. Two long-lived states were found in both experiments with (i) $T_{1/2} = 8.7$ s and $I^\pi = 1^+$ and (ii) $T_{1/2} = 49.2$ s and $I^\pi = 8^+$ [64]. Following Q-value measurements in coincidence with γ rays in ^{90}Mo the shorter-lived 1^+ component was assigned to the ground state [64]. The excitation energy of the 49.2-s level was deduced in the AME2003 [55] employing the data from Iafigliola [63] and Oxorn [64], with the earlier being a measurement without a β-γ coincidence. Here, the branching ratio to the 948-keV (2^+) level in ^{90}Mo is 22% in contrast to Oxorn and Mark [64], which give log ft values that are vice versa. With a branching of 78% [64], the excitation energy to be derived from these data is 124(390) keV instead of 310(390) keV [37].
In two other experiments, ^{90}Tc was produced via the fusion-evaporation reaction ^{58}Ni(^{36}Ar, 3pn) at 149 MeV beam energy [65] and as a decay product of laser-ionized ^{90}Ru produced in ^{58}Ni(^{36}Ar, 2p2n)^{90}Ru reactions at 180 MeV beam energy at the LISOL facility [39]. In the latter experiment only low-spin states of ^{90}Tc were populated in the β decay of ^{90}Ru ($I^\pi = 0^+$), while in the earlier in-beam experiment no low-spin state could be observed. This behavior agrees with the expectation that in fusion-evaporation reactions states at high spin and excitation energies up to several MeV are populated due to their high geometrical cross sections [66]. Thus, a considerable amount of the flux populates high-spin states.
Rudolph *et al.* [65] refer to this level as the ground state, supported by the observation from experimental spin assignments in the neighboring odd-odd nuclides ^{88}Nb ($N = 47$), ^{90}Nb ($N = 49$), ^{92}Tc ($N = 49$), and the predictions from shell-model calculations.
In Dean *et al.* [39] the β decay of ^{90}Ru was studied and the low-spin and high-spin level schemes from shell-model calculations were compared with experimental results. In conclusion, these calculations are also suggesting a high-spin ground state for ^{90}Tc.
Our production mechanism via fusion-evaporation reactions would also favor the production of the high-spin isomer. A careful examination of the SHIPTRAP data using the count-rate class analysis [47] shows no evidence of a possible contamination in the trap, even regarding a smaller excitation energy. For these reasons we clearly assign the measured mass value to the 8^+ level.
Within the $N = 47$ chain several new Penning trap measurements were conducted in this work for the isotones from ^{87}Zr ($Z = 40$) to ^{92}Rh ($Z = 45$) (see Fig. 3). In the attempt to interpolate the mass value for ^{93}Pd, the two-proton separation energies derived from these data were plotted. Figure 5 shows a smooth systematic behavior after the assignment of our mass value to the ground state of ^{90}Tc according to the justification given in Ref. [65]. If our mass value were assigned to the excited isomeric state [55, 64], the smooth trend is interrupted. We therefore regard the first possibility as the more probable one. However, considering the prevalent discrepancies among the available literature this nuclide should be addressed in a future measurement.

^{88}Tc: This nuclide was first identified in in-beam γ-ray studies after fusion-evaporation reactions. A study of the ^{58}Ni(^{36}Ar, αpn)^{88}Tc reaction at a beam

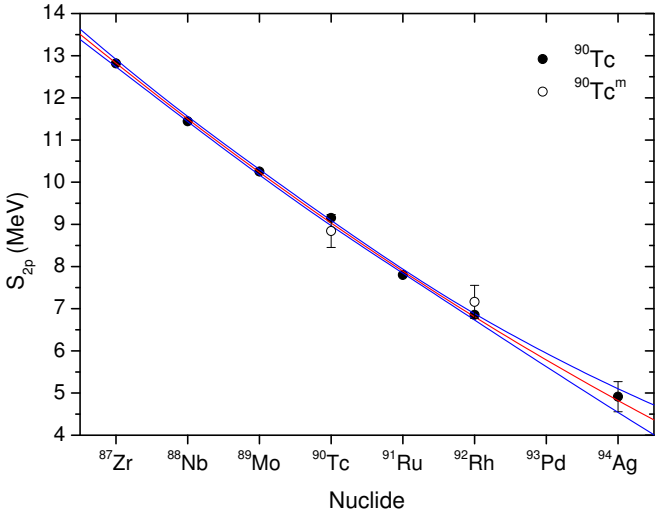

FIG. 5: Plot of two-proton separation energies for $N = 47$ isotones. The binding energies for ^{85}Sr and ^{86}Y were taken from AME2003 and the value for ^{94}Ag was derived from the Coulomb displacement energy and the newly-determined mass of ^{94}Pd. S_{2p} energies with our mass value assigned to the ground or isomeric state of ^{90}Tc are indicated. This diagram is discussed in a dedicated publication on the decay modes in ^{94}Ag [67].

energy of 145 MeV was conducted at the VICKSI accelerator at the HMI/Berlin. After an annihilation-γ-coincidence measurement of the 7^- (3350 keV) and the 8^+ (3212 keV) yrast states in ^{88}Mo, the ground state was suggested to have a spin/parity of either 7^- or 8^+ [68]. Gamma radiation in ^{88}Mo following the β decay of a low-spin state in ^{88}Tc has not been observed in Ref. [69]. In a β-decay study at the Tandem Accelerator Laboratories at Kyushu and Tsukuba using the ^{58}Ni(^{32}S, pn)^{88}Tc reaction [70] two β-decaying states with half-lives of 5.8(0.2) s for a low-spin state $(2, 3)^+$ and 6.4(0.8) s for a high-spin state $(6, 7, 8)$ were observed in coincidence with γ rays. The β-decay endpoint energies were measured by β-γ coincidence gated on the 741-keV γ ray and the derived $Q_{\rm EC}$ values of ^{88}Tc were given in two different papers [70, 71]. In both cases these values are significantly lower by 1.4 MeV and 2.2 MeV, respectively, than those from the systematic trends. Therefore, this Q value has been replaced by a systematic value in AME2003. Our mass excess value of $-61679.1(3.8)$ keV determined with JYFLTRAP is even less bound than the systematic value by 1030 keV. In analogy to the neighboring odd-odd nuclide ^{90}Tc we have most probably determined the mass of the high-spin state. Since the positions of the ground and isomeric states are identical according to extrapolations (see Table I) a treatment for an unknown mixture of states [61] cannot be applied and our result is assigned as the ground state mass with an increased uncertainty of 87 keV.

^{90}Ru, **^{92}Ru**, **^{92}Rh**, and **^{93}Rh**: The measurements reported here are the first experimental mass determinations of these nuclides. The even-even ruthenium isotopes have 0^+ ground states and in ^{93}Rh no isomeric state was observed. All data identify the nuclei less bound than suggested, based on the extrapolation from systematic trends in AME2003 [55]. ^{92}Rh and ^{92}Ru are less bound by 361 keV and 111 keV, respectively. For ^{90}Ru a mass difference of 427 keV deviates by 1.4σ from the systematic estimates of the AME2003. These observations continue the trends in the $A = 90$ and $A = 92$ chains along the isobaric distance from stability. ^{93}Rh is less bound by 159 keV. Here, the general observation of less bound experimental mass values is continued.
Evidence for a possible existence of another long-lived state in ^{92}Rh is given in a publication by Dean *et al.* [39]. Since observed feedings to the low-spin (0^+, 2^+) levels in the daughter ^{92}Ru are larger than expected when originating from the presumed ($\geq 6^+$) ground state, a low-spin isomeric state might exist. Indeed, a second half-life component was observed in the 866-keV γ-ray line, with a deduced half-life of 0.53 s. According to shell-model calculations a 2^+ state is predicted either about 50 keV [39, 72] or 211 keV [73] below the 6^+ state. A total duration of our Penning trap measurement of 1.7 s resulted in a disintegration of most of the shorter-lived isomeric component, if it were produced, and our mass value is hence assigned to the high-spin isomer. In addition, the high-spin states are more favorably produced via heavy-ion fusion-evaporation reactions. In order to account for the unknown level scheme between the ($\geq 6^+$) and the 2^+ states, the uncertainty of the ground-state mass excess value of ^{92}Rh is increased to 15 keV. Spectroscopic experiments are required to confirm the low-energy level scheme of this nuclide which is of vital importance for the study of the two-proton decay of ^{94}Ag (21^+) [67, 74, 75, 76, 77].

^{94}Ru, **^{96}Pd**: In both nuclides the 0^+ ground state and an 8^+ isomeric state with an excitation energy larger than 2.5 MeV were observed in previous measurements. Due to their μs half-lives, nuclides in the latter states have no influence on a cyclotron frequency measurement. In AME2003 the ground state mass values are ultimately related to the mass of the primary nuclide ^{96}Ru. The mass of ^{94}Ru was previously determined with an uncertainty of 13 keV in the ^{96}Ru(p,t) reaction [78]. The combined result from the Penning trap experiments agrees within one standard deviation to the previously measured value.
The mass of ^{96}Pd was previously determined via its β decay [79] and the ^{96}Ru(p,n)^{96}Rh reaction [80] Q values. Its uncertainty of 150 keV is dominated by the decay measurement. According to our new experimental mass value, with a 30-fold improved precision, the nucleus is by 51 keV less bound.

Nuclides with assigned spin values $I^\pi = 9/2^+$ and $I^\pi = 1/2^-$ for the ground and first isomeric state, respectively: ^{87}**Zr**, ^{89}**Mo**, ^{89}**Tc**, ^{91}**Tc**, ^{91}**Ru**, ^{93}**Ru**, and ^{95}**Rh**: In most cases the half-lives of the ground and isomeric states are very similar or at least sufficiently long to allow for a measurement of both states. The sole exception is ^{89}Mo^m, with a half-life of the excited isomer of 190 ms. The excitation energies of ^{89}Tc^m and ^{91}Ru^m are well below the employed experimental resolution of the present experiments of $\Delta m = 120$ keV for SHIPTRAP or $\Delta m = 80 - 90$ keV for JYFLTRAP. Despite the fact that there is a difference of only four spin units between the isomeric state and the ground state, instead of seven for ^{90}Tc, we assume that the high-spin-state products are favored due to the fusion-evaporation mechanism. This fact, combined with the results obtained in the count-rate class analysis for ^{89}Mo, ^{91}Tc, or ^{93}Ru which give no indication of an additional admixture by a different mass, supports the assignment of the mass values of these species to the high-spin ground states.

^{87}**Zr**: The result from JYFLTRAP agrees with the AME2003 value for the ground state, which is derived from the mass of ^{90}Zr and the ^{90}Zr(^{3}He,^{6} He)^{87}Zr reaction Q value, determined at MSU [81]. However, our value deviates by 1.5 standard deviations from the result $ME = -79384(28)$ keV of an ESR Schottky measurement [82], which is not used in the adjustment procedure of the Atomic Mass Evaluation due to its higher uncertainty.

^{89}**Mo**: The value from JYFLTRAP agrees with the AME2003 value, which is determined via a reaction Q-value measurement ^{92}Mo(^{3}He,^{6} He)^{89}Mo from a study at MSU [83] and the mass of the primary nuclide ^{92}Mo.

^{89}**Tc**: For ^{89}Tc a Q_β measurement was performed by Heiguchi *et al.* [84] yielding a mass excess of $ME = -67500(210)$ keV. However, AME2003 assumed this value to be lower by 350 keV than given by this experiment due to its difference to other experimental results in this region. Our combined result of $ME = -67394.8(3.7)$ keV lies 445 keV above the value suggested by systematics in AME2003 and is in full agreement with [84], although 30 times more precise. Since a pure production of the high-spin state is assumed, a correction for an isomeric mixture, $E_{\rm ex} = 62.6$ keV [85], is not applied.

^{91}**Tc**: This nuclide has an isomeric state with a well-known excitation energy of $E_{\rm ex} = 139.3(3)$ keV, which is sufficiently large to be resolved in the present measurements at SHIPTRAP and JYFLTRAP. Since no count-rate-dependent effects were observed, we assume the pure presence of ions in the $9/2^+$ ground state. The Q_β-decay energy of ^{91}Tc produced in a (p,2n) reaction at 30 MeV beam energy [63] resulted in a mass excess value of $-75980(200)$ keV, which is in good agreement with our result, but 60 times less precise.

^{91}**Ru**: The mass of ^{91}Ru was previously unknown. In AME2003 it was deduced from the known mass of its isomer, using an estimated excitation energy of 80(300)# keV. Due to the high uncertainty in the isomeric excitation energy, it cannot be definitely concluded that ground and isomeric states were resolved in the measurement, although a mass resolution of $\Delta m = 80$ keV was employed at JYFLTRAP. Here, no count-rate-dependent effects were observed in the analysis. Our averaged result for ^{91}Ru combined with the mass of the isomer, which was obtained by Hagberg [86] from delayed proton-(ϵp)-decay-energy measurements, now locates the excited state at -340(500) keV. Given the large uncertainty in this value the assignment of the isomeric state in this nuclide is still ambiguous. However, Hagberg clearly states that the value they obtained for the (ϵp) decay energy was only a lower limit. If we assume this energy to be by 500 keV higher than the actual value of 4300(500) keV [86], then the excitation energy would be +160 keV.

^{93}**Ru**: In this nuclide the two lowest states have sufficiently long half-lives for both to be delivered to the JYFLTRAP Penning trap setup. Since the excitation energy is 734.4(1) keV and precisely known, the ground and isomeric states can in principle be resolved with a mass resolution Δm of 85 keV.
The derived mass excess value agrees well with the value for the $9/2^+$ ground state, which is determined from a Q_β measurement via ^{93}Tc and a (p,γ)-reaction Q value to the stable nuclide ^{92}Mo [87]. The uncertainty in this mass value is now improved by more than a factor of 20.

^{95}**Rh**: This nuclide has been studied in γ-γ and β-γ coincidence measurements at the McGill synchrocyclotron [88]. A 5-min ground state and a 2-min isomeric state have been observed. Additionally, the isomeric transition between the $1/2^-$ and the $9/2^+$ states has been identified. From the β-endpoint energy, the Q value and the mass excess have been derived with an uncertainty of 150 keV. In the ^{40}Ca + ^{58}Ni reaction, as employed in this experiment, the high-spin state is more likely to be produced. This assumption is supported by the study of neutron-deficient ruthenium and rhodium isotopes produced with the same reaction at the Munich tandem and heavy-ion post accelerator [89]. In that work, the $1/2^-$ state has been only weakly populated at a beam energy of 135 MeV, whereas a strong production of the $9/2^+$ ground state has been observed.
Similar to the situation of ^{93}Ru, the mass value determined by JYFLTRAP is in excellent agreement with the previous value of the $9/2^+$ ground state, but now with more than 35-fold lower uncertainty compared with the previous result stemming from Q_β decay to the primary nuclide ^{95}Ru [90].

^{92}Tc: Our averaged mass excess value of $ME = -78924.7(3.7)$ keV is found to be in good agreement with all former measurements from studies using either (p,n) or (^{3}He,t) reactions [91, 92].

^{94}Rh: In this nuclide, two states are reported in NUBASE (see Table I) with tentatively assigned spin values of $(2^+, 4^+)$ and (8^+) for the 71-s ground and 26-s isomeric states, respectively. Their relative order is, however, uncertain since the ground-state mass value is only estimated from systematic trends and the one of the excited isomeric state is determined via the Q value to ^{94}Ru [61], based on a β-endpoint measurement for the 71-s low-spin state, referred to (3^+) in Ref. [93]. Despite the high uncertainty in the excitation energy of $E = 300(200)\#$ keV, a value which is estimated from systematic trends [131], we can assume to have resolved both states with a mass resolution of $\Delta m = 86$ keV.
An experiment studying β-delayed proton emission, conducted at the on-line mass separator [94] at GSI/Darmstadt, observed that the 26-s ^{94}Rh activity did not show any grow-in effect [95]. It was deduced that this state was probably directly produced in the employed ^{40}Ca + ^{58}Ni reactions and released from the ion source, whereas the observed low-spin 71-s state was fed from the β decay of ^{94}Pd. In addition, a recent study on low-lying levels in ^{94}Ru following the identical reaction [96] concluded that the (4^+) state had not been significantly populated. Hence, we tentatively assign our measured mass value to the (8^+) high-spin state.
A recent $Q_{\rm EC}$-value determination of ^{94}Pd and of the 71-s state in ^{94}Rh was carried out at the GSI on-line mass separator after fusion-evaporation reactions (^{40}Ca on ^{58}Ni) employing the Total Absorption Spectrometer (TAS) [97]. Here, the activity of the latter state was produced as a daughter of the ^{94}Pd β decay.
The results on $Q_{\rm EC}$ values of the ^{94}Pd and ^{94}Rh decays are summarized in Fig. 6. Both decay experiments studied the 71-s component and their weighted average is given. The summed $Q_{\rm EC}$ values for both nuclides, derived from JYFLTRAP mass values and involving the high-spin (8^+) state in ^{94}Rh, agree with the mass difference between ^{94}Pd and ^{94}Ru. The comparison of these data indicate an energetic ordering with an (8^+) ground state, in accordance with shell-model calculations [73]. Although this comparison is governed by large uncertainties in the Q-value determinations, we tentatively assign our result to the ground state. A similar conclusion was already drawn in Ref. [97] after a comparison with the mass excess value by the Canadian Penning Trap for ^{94}Rh, using fusion-evaporation reactions with heavy-ion beams at ANL [56].

^{94}Pd: Since the excited isomeric state possesses a half-life in the nanoseconds range, a clean sample of ions in the ground state has been delivered to the experiment. The mass of this 0^+ state with a half-life of 9 s is determined experimentally for the first time. It agrees with the value of the AME2003 derived from the extrapolation of systematic experimental trends.

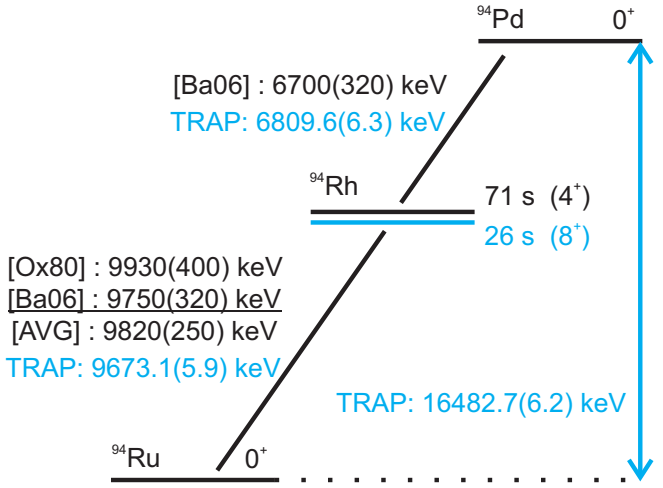

FIG. 6: $Q_{\rm EC}$ values of the ^{94}Pd and ^{94}Rh decays, measured at the Foster Radiation Laboratory (Ox80) [93], the GSI on-line mass separator (Ba06) [97], and within this work (TRAP). Both decay experiments studied the 71-s (4^+) isomeric component and their weighted average is given. The $Q_{\rm EC}$ values from JYFLTRAP for these $A = 94$ nuclides involve the (8^+) isomeric state in ^{94}Rh.

^{95}Pd: The nuclide ^{95}Pd has been produced in the fusion-evaporation reaction $^{\rm nat}$Ni(^{40}Ca, 2pxn)^{95}Pd with a predicted cross section [98] on the order of a mb at an energy about 145 MeV. Since the RF-excitation time for the radial motions in the trap was 800 ms and the half-lives are sufficiently long, nuclides in their ground and isomeric states were observed in the measurement. Indeed, cyclotron resonance curves at two different frequencies were recorded.
The long-lived isomeric state ^{95}Pd^m with a half-life of 13.3(3) s was observed in investigations of β-delayed proton emission [99] and β decay [95]. The spin value of this state whose β-p chain strongly feeds the 8^+ state in ^{94}Ru was assigned as $21/2^+$ [99] in accordance with the shell-model predictions [100]. The interpretation of this state as a spin-gap isomer is based on the long-lived character of the decay [99] and on the observation of the weak palladium K X-rays at mass $A = 95$ [95].
Moreover, the exact position of the $21/2^+$ state will determine the energies of high-spin yrast states up to $43/2^+$ built on this isomer [101, 102]. The value for the ground-state mass excess is $-69961.6(4.8)$keV and for the isomeric state it is $-68086.2(4.7)$ keV. Using these directly measured values we determined the excitation energy of the isomeric state as $E = 1875.4(6.7)$ keV. This is the first direct mass determination of such a high spin state. The value is in excellent agreement with the one of 1875 keV, obtained from γ-decay spectroscopy [101]. Our new experimental result can be compared

with the theoretical predictions of 1.9 MeV [100], 1.8 MeV [102], 1.97 MeV [103] and with evaluated data 1.86(50)# MeV of the AME2003 [37]. Recently, the energy of this isomeric state was determined from the γ transitions which connect the states built on the ground and isomeric states [104] to 1876 keV, in agreement with our value. The latter work concludes that the $21/2^+$ state lies lower than the $15/2^+$, $17/2^+$, and $19/2^+$ states, manifesting its spin-gap character of isomerism. Hence, the excitation energy confirms the spin-gap character expected from the shell-model calculations taking into account the inert ^{100}Sn core and, therefore, indirectly confirming the magic character of the nuclide with $Z = N = 50$.

The Q_{EC} value for the isomeric state is equal to 10256.1(6.3) keV. The β decay of the isomeric state dominantly feeds the 2449-keV $(21/2^+)$ level in ^{95}Rh [95], which results in a transition Q value of 8829(6.3) keV. Taking into account a decay branching of 35.8% [95], we obtain a log $ft = 5.5$, confirming the allowed character of the transition.

VI. OBSERVATIONS IN NUCLEAR STRUCTURE

The two-neutron separation energy $S_{2\mathrm{n}} = B(Z,N) - B(Z,N-2)$ is the mass derivative which best represents the systematic behaviour of the studied binding energies and the nuclear structure evolution around the well-established $N = 50$ shell closure. Figure 7 shows the $S_{2\mathrm{n}}$ values of the isotopes from selenium to cesium. The data available in AME2003 (grey circles) have been complemented by new experimental data (black circles) from JYFLTRAP [31], SHIPTRAP [32] and this work. For the lowest neutron numbers, data points are partly combined with AME2003 values that are based on experimental input data. In addition to the expected decrease of the $S_{2\mathrm{n}}$ energies with increasing neutron number the well-established $N = 50$ shell closure is observed.

The region with neutron numbers $N \geq 50$, which was previously partly established by experimental results, is well reproduced by the data from Martín *et al.* [32]. In contrast, the region below this neutron-shell closure, which was based mostly on extrapolations of systematic trends, is substantially modified for isotopes from technetium to palladium. The separation energies are now solely defined by experiment and all values are shifted consistently towards higher energies comprising equidistant lines of similar curvatures.

Comparing the changes in the two-neutron separation energies for the isotopes of niobium and molybdenum at neutron numbers $N = 46$ and $N = 47$ [132] two observations are made: (1) both experimental data points of the AME2003 for molybdenum are still well reproduced after including our mass values for ^{88}Mo and ^{89}Mo, (2) a shift of the separation energies towards higher values is observed in niobium. The mass values of these nuclides are now entirely determined by JYFLTRAP data, whereas the previous AME2003 data were based on Q_β measurements. Note that the contribution of known, but unobserved, isomers has been accounted.

The $S_{2\mathrm{n}}$ data point for ^{85}Nb at $N = 44$ is calculated using the masses of the nuclides ^{85}Nb and ^{83}Nb, which were previously mainly determined by sequences of β-decay endpoint measurements up to degrees [133] 5 and 4, respectively [37]. The possibility of too low mass values due to unobserved γ lines can in theory be attributed to any of the contributing results. Triggered by an inconsistency in the Q_β value for ^{85}Nb given in Ref. [105], the AME2003 mass value was recalculated and is now shifted by 70 keV to a less bound value (light grey circle).

Furthermore, the presence of long-lived isomeric states can obscure the interpretation of results from mass measurements. Along either of the $A = 83$ and $A = 85$ chains two isobars, ^{83}Zr, ^{83}Y and ^{85}Nb, ^{85}Zr, were studied with the JYFLTRAP mass spectrometer, but due to the open question of the isomeric mass-to-state assignment for ^{83}Y and ^{85}Nb [31] a correction for a mixture between two states has been applied.

Departing from stability along the $A = 83$ chain, the mass values from JYFLTRAP identfy the nuclei less bound by 130 and 552 keV for ^{83}Y and ^{83}Zr, respectively. Hence, the mass value for ^{83}Nb is also expected to be less bound by at least 682 keV compared with the present AME2003 value. For the isotope containing two more neutrons, ^{85}Nb, the question of an isomeric mass-to-state assignment is not solved and a state with an isomeric excitation energy of 69 keV is reported in Ref. [31]. These are considered and combined with a modified mass value for ^{83}Nb and illustrated by a black upfacing triangle, in agreement with the rather large uncertainty of the AME2003 value determined by Ref. [105]. Due to these open questions of isomerism this region should be addressed in a future measurement for final unambiguous mass-to-state assignments. Ideally, the cyclotron frequency determinations should be assisted by either a hyperfine-state-selective laser ionization [106, 107] or a nuclear decay-spectroscopy experiment [108].

In Fig. 8 the two-neutron separation energies $S_{2\mathrm{n}}$ are displayed as a function of the proton number for even isotones across the $N = 50$ shell gap. This gap $\Delta_n(N = 50)$ is defined as the difference between the two-neutron separation energies for $N = 50$ and $N = 52$, noticeable in Fig. 7 as the steepness of the slope and in Fig. 8 as a gap between $N = 50$ and $N = 52$. In addition to the neutron-deficient data described in this work, Penning trap data from JYFLTRAP [49, 109, 110] and ISOLTRAP [111] contribute to delineate the position of the shell gap on the neutron-rich side. A minimum in the shell-gap energy was observed for $Z = 32$ in Ref. [109] with an indication of an enhancement towards the doubly-magic ^{78}Ni ($Z = 28$).

In the lower set of lines above the magic shell closure, a very regular behavior is observed for isotopes beyond

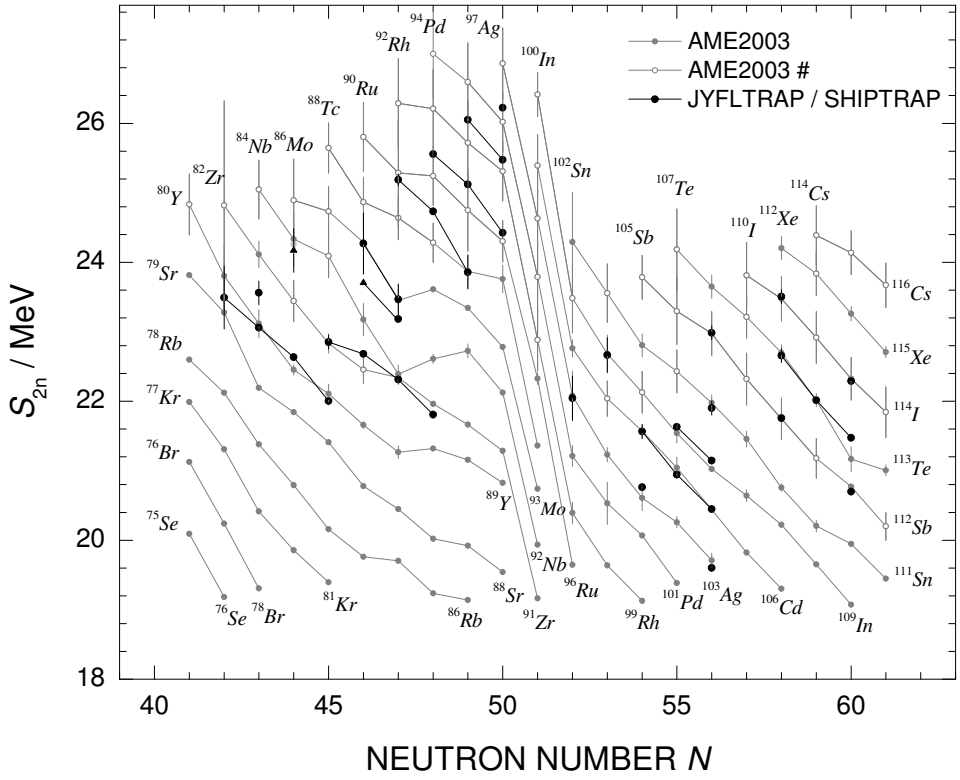

FIG. 7: Two-neutron separation energies S_{2n} derived from this work (black circles) and AME2003 (grey circles). The data points of AME2003 are either based solely on experimental results (filled circles, AME2003) or at least partly derived from extrapolations of systematic trends (open circles, AME2003 #). The data points for ^{85}Nb and ^{87}Nb (triangles) imply a correction due to the presence of an isomeric state. For a detailed discussion see text.

molybdenum ($Z \geq 42$), indicating the rigidity of the $N = 50$ shell gap towards ^{100}Sn, whereas an increasing difference develops between the $N = 56$ and $N = 58$ isotones below niobium ($Z \leq 41$). This is in accordance with the developing shape change at $N = 59$ for niobium, zirconium [112, 113], and yttrium [114]. Contrary to this, the regular line spacing is visibly compressed for the yttrium isotopes at mid-proton shell ($Z = 39$).

Many of the studied nuclides play a role in the astrophysical rp- and νp-processes and their proton-capture rates and finally the isotonic abundance ratios are influenced by our mass data (see Fig. 3). In consequence of these measurements, which are partly the first experimental determinations, the one-proton separation energies are now more accurately known. This is illustrated in Fig. 9 for elements from yttrium to silver as a function of the isotopic distance from the $N = Z$ line. The one-proton separation energies S_p of more than 45 nuclides have been modified by the new experimental data and those from Ref. [31]. Since these often affect both mass values, $m(A, N)$ and $m(A-1, N)$, by a similar amount, the resulting corrections in the separation energies are partly canceled out. Nevertheless, the reduction of experimental uncertainties by more than a factor of ten provides a rectified set of input data for astrophysical calculations and will result in a more reliable modeling of the pathways, since in previous network calculations values with large uncertainties and assumptions based on extrapolations have been used.

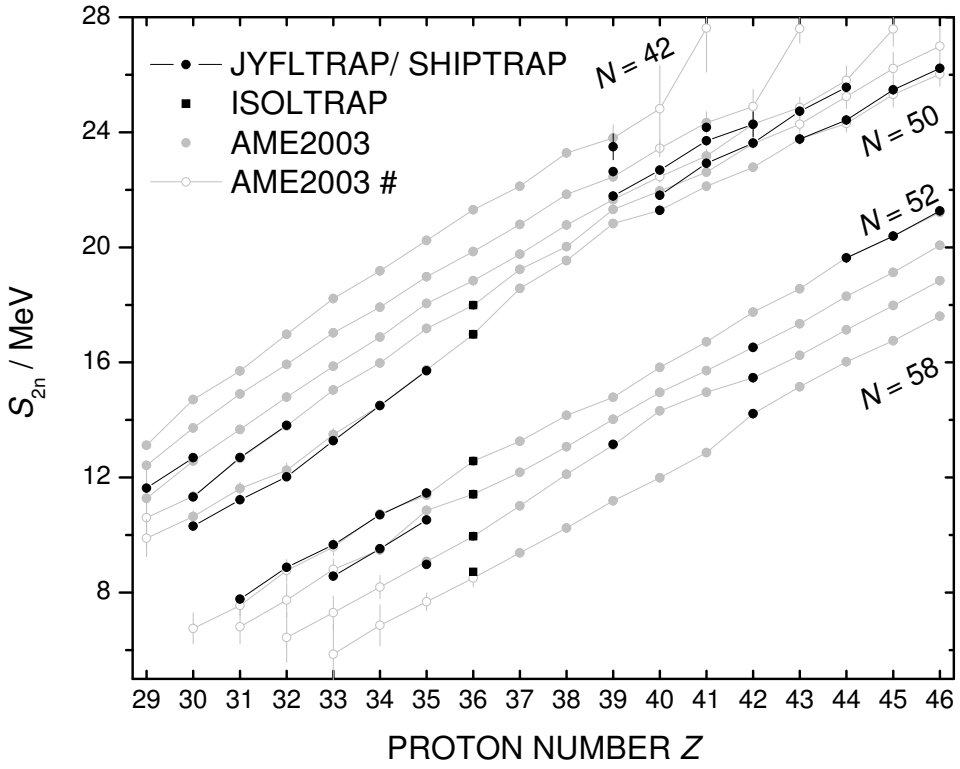

FIG. 8: Two-neutron separation energies S_{2n} as a function of the proton number for even isotones across the $N = 50$ shell gap. The data points of AME2003 are either based solely on experimental results (filled circles, AME2003) or at least partly derived from extrapolations of systematic trends (open circles, AME2003 #). The data of krypton isotopes ($Z = 36$) are from Ref. [111] (black squares). The data points for ^{85}Nb and ^{87}Nb imply a correction due to the possible presence of an isomeric state (compare Fig. 7).

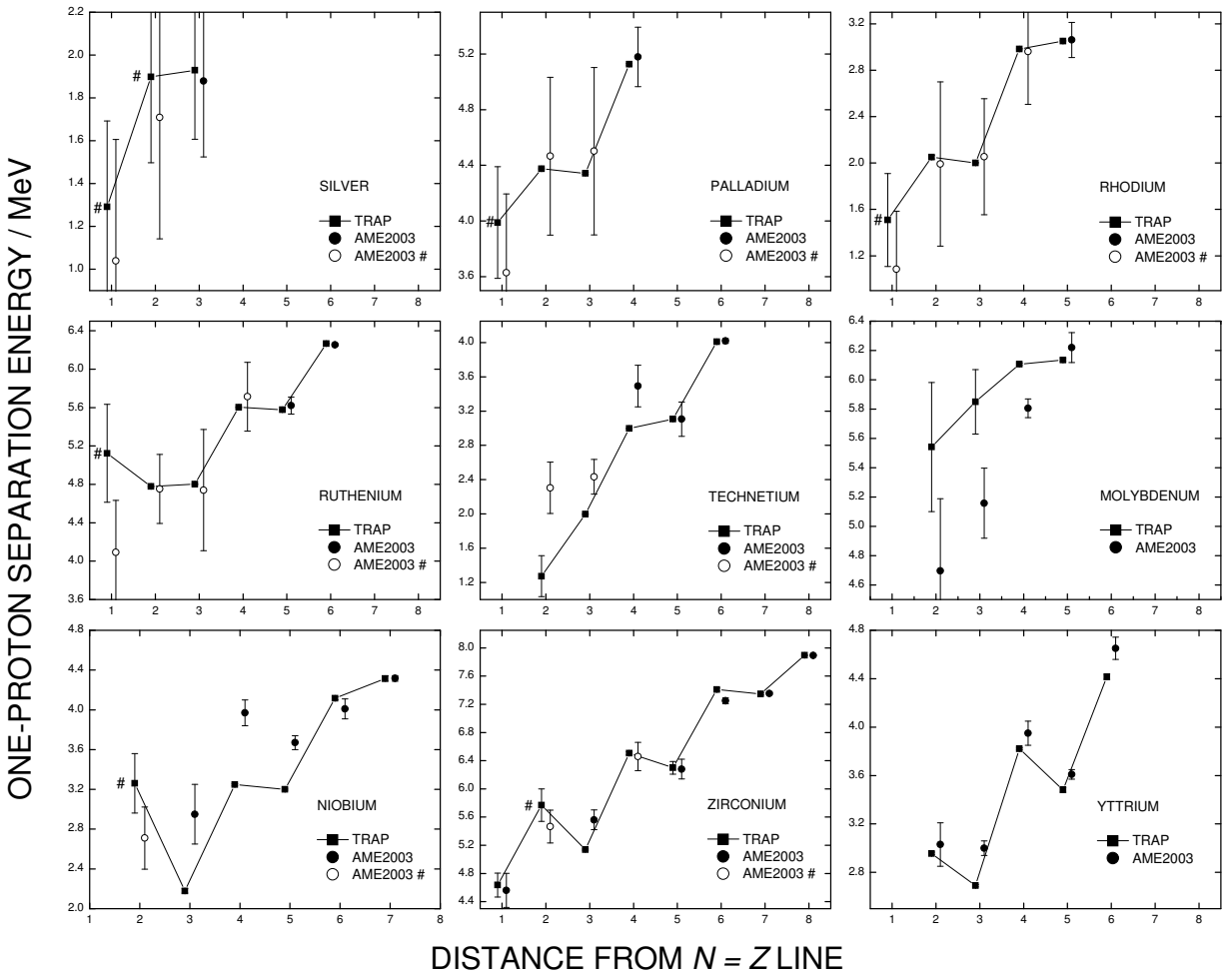

FIG. 9: One-proton separation energies as a function of the distance from the $N = Z$ line for the isobars from yttrium to silver. The data points of AME2003 are either based solely on experimental results (filled circles, AME2003) or at least partly derived from extrapolations of systematic trends (open circles, AME2003 #). The trap data result in major adjustments of some of the values and moreover in a considerable reduction of the error bars. Separation energies S_p comprising data from ^{83}Y or ^{85,87,88}Nb were corrected for the possible presence of an unknown isomeric contribution. For some of the nuclides the separation energies are a combination of a trap measurement and a value of the AME2003 and hence exhibit a larger uncertainty. These are $^{80-84}$Y, $^{81,82,86-88}$Zr, ^{84,89}Nb, ^{86,87}Mo, ^{88,91,92}Tc, ^{89,94}Ru, ^{91}Rh, ^{93}Pd, and $^{95-97}$Ag. In addition, data combined with extrapolated AME2003 values are marked by '#'.

VII. IMPLICATIONS FOR ASTROPHYSICS

The neutron-deficient nuclei measured in this work are located in the paths of two astrophysical nucleosynthesis processes: the rp-process [30, 115] and the recently discovered νp-process [11, 12, 13] (see Fig. 3). In the following, we will investigate the implications of the newly-determined mass values on the reaction flow and the nucleosynthesis yields of the νp-process. A similar investigation for the rp-process will be subject of a forthcoming paper.

The νp-process occurs in explosive environments when proton-rich matter is ejected under the influence of strong neutrino fluxes. This includes the inner ejecta of core-collapse supernova [116, 117, 118] and possible ejecta from black hole accretion disks in the collapsar model of gamma-ray bursts [119]. The matter in these ejecta is heated to temperatures well above 10 GK and becomes fully dissociated into protons and neutrons. The ratio of protons to neutrons is mainly determined by neutrino and antineutrino absorptions on neutrons and protons, respectively. As the matter expands and cools, the free neutrons and protons start to form α particles. Later, at temperatures around 5 GK, α particles assemble into heavier nuclei but the expansion of matter is so fast that only a few iron-group nuclei are formed. Once the temperature reaches around 2 GK the composition of the ejecta consists – in order of decreasing abundance – mostly of ^{4}He, protons, and iron group nuclei with $N \sim Z$ (mainly ^{56}Ni).

Without neutrinos, the synthesis of nuclei beyond the iron peak becomes very inefficient due to bottleneck nuclei (mainly even-even $N = Z$ nuclei) with long β-decay half-lives and small proton-capture cross sections. However, during the expansion the matter is subject to a large neutrino and antineutrino flux from the proto-neutron star.

While neutrons are bound in neutron-deficient $N = Z$ nuclei and neutrino captures on these nuclei are negligible due to energetics, antineutrinos are readily captured both on free protons and on heavy nuclei on a timescale of a few seconds. As protons are more abundant than heavy nuclei antineutrino captures occur predominantly on protons, leading to residual neutron densities of 10^{14}–10^{15} cm^{-3} for several seconds. These neutrons are then easily captured by the heavy neutron-deficient nuclei, for example ^{64}Ge, inducing (n,p) reactions with time scales much shorter than the β-decay half-life. Now proton captures can occur on the produced nuclei, allowing the nucleosynthesis flow to continue to heavier nuclei. The νp-process [11] is this sequence of (p,γ) reactions followed by (n,p) or β^+-decays, where the neutrons are supplied by antineutrino captures on free protons.

Here, the impact of the new mass measurements on the νp-process nucleosynthesis is studied in post-processing calculations of a representative trajectory from the explosion of a 15 M$_\odot$ star [120]. This trajectory is characterized by efficiently synthesizing nuclei with $A > 90$ and is the same as used in Refs. [12, 121]. The neutrino temperatures and luminosities are assumed to remain constant at the values reached at 1000 ms postbounce. With this assumption our results are directly comparable to those from Ref. [12].

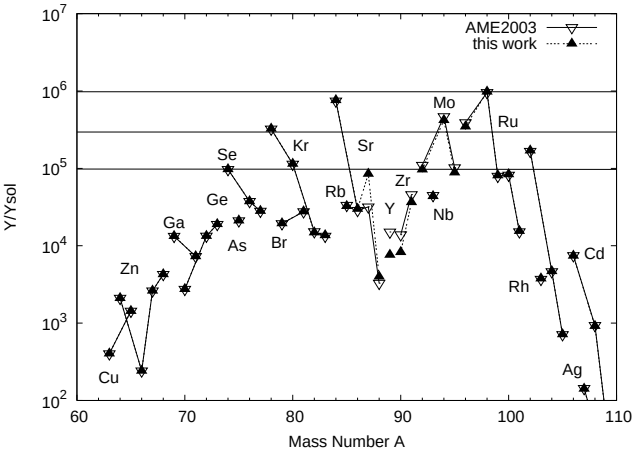

FIG. 10: Final abundances after decay to stability relative to solar abundances [126]. Filled upfacing triangles are for a calculation using the masses studied here. Open downfacing triangles are for a calculation using AME2003 masses.

Two sets of astrophysical reaction rates were used in the reaction network. A reference set [122] included theoretical rates obtained with a new version of the NON-SMOKER code [123]. The theory is similar to previous calculations [124] but containing a number of updates and improvements, among which the latest information on excited states [125] and masses from the AME2003 [55] are the most important in the current context. To consistently study the impact of the new mass data, a second rate set was prepared, similar to the reference set except for the inclusion of mass values from this work and Ref. [31]. It has to be noted that we did not only change the reaction Q values but consistently recalculated the theoretical rates with the newly implied separation energies.

Figure 10 shows the final abundances normalized to solar abundances after decay to stability for the two sets of thermonuclear reaction rates. Only nuclei produced in the p-rich ejecta are shown. As is clearly seen from the figure there is no difference in the yields for the two different sets of rates except for a few nuclei in the mass range $85 < A < 95$, namely for ^{87,88}Sr, ^{89}Y, and ^{90,91}Zr. This can be directly traced back to the large change in the mass of ^{88}Tc ($\Delta ME_{\mathrm{AME2003-TRAP}} = -1031$ keV, see Table II). This change in mass leads to an increase in the reaction rate for ^{88}Tc$(\gamma,\mathrm{p})^{87}$Mo at the relevant temperatures and therefore a relative suppression of the flow through ^{87}Mo(p,γ)^{88}Tc.

Figures 11 and 12 show the time-integrated reaction flows relative to the 3α-reaction employing the mass data from AME2003 only and the mass data from AME2003 with the addition of the new results, respec-

tively. In the case of reaction rates employing the newly-determined mass values, the main reaction flow to nuclei with $A > 88$ proceeds through ^{87}Mo(n,p) ^{87}Nb(p,γ) ^{88}Mo(p,γ) ^{89}Tc. In comparison, for reaction rates based on the AME2003 masses the flow through ^{87}Mo(p,γ)^{88}Tc is not suppressed. This opens up two additional paths for significant reaction flows: ^{88}Tc(n,p)^{88}Mo(p,γ)^{89}Tc and ^{88}Tc(p,γ)^{89}Ru(n,p)^{89}Tc. In consequence, the reaction flow of the previous case, ^{87}Mo(n,p)^{87}Nb(p,γ)^{88}Mo(p,γ)^{89}Tc, becomes weaker. When examining the reaction flows (Figs. 11 and 12) in detail one notices a flow through ^{87}Nb(n,p)^{87}Zr in the case of the newly-determined mass values (see Figure 12). This is a consequence of a stronger reaction flow through ^{87}Mo(n,p)^{87}Nb and thus a higher abundance of ^{87}Nb compared to the calculation using the AME2003 masses only. This is seen in the final abundances after decay as increased abundance of ^{87}Sr (see Fig. 10). Similarly, the relative suppression of the flow through ^{88}Tc(p,γ)^{89}Ru(n,p)^{89}Tc in the calculation using the newly-determined mass values of this work leads to the observed lower abundance of ^{89}Y. The change in the mass of ^{90}Tc leads to a slight increase in the reaction rate for ^{90}Tc(γ,p)^{89}Mo, thus shifting some mass of the $A = 90$ chain into the $A = 89$ chain. As a result, the final abundance of ^{90}Zr is lower for the calculation employing the newly-determined mass values of this work.

When comparing the reaction flows in Fig. 11 and Fig. 12 it seems that the newly-determined mass values allow an additional flow through ^{92}Rh(p,γ)^{93}Pd(n,p)^{93}Rh. However, this is an artefact due to the discrete bins of the reaction flows for plotting purposes. For the calculation based on the AME2003 mass data these flows are just slightly below the bin threshold (1% of the flow through the 3α-reaction). The total flow reaching ^{94}Pd is very similar in both cases, only the relative strength in the two paths, ^{92}Rh(p,γ)^{93}Pd(n,p)^{93}Rh and ^{92}Rh(n,p)^{93}Rh(p,γ)^{93}Rh is different.

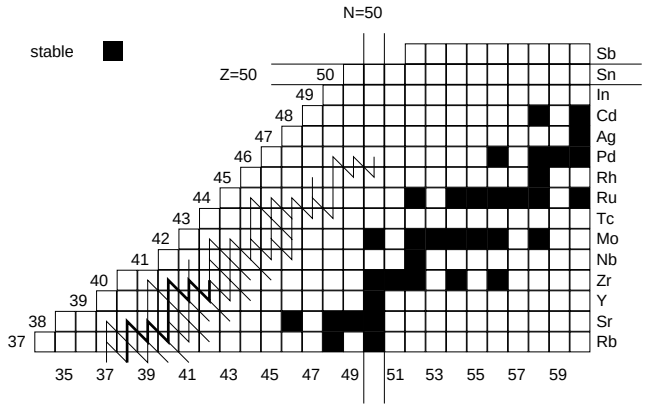

FIG. 11: The time-integrated reaction flow for the νp-process using the reaction rate set based on the AME2003 mass data only. The reaction flows shown are more than 10% (thick line) and 1–10% (thin line) of the reaction flow through the triple-α-reaction.

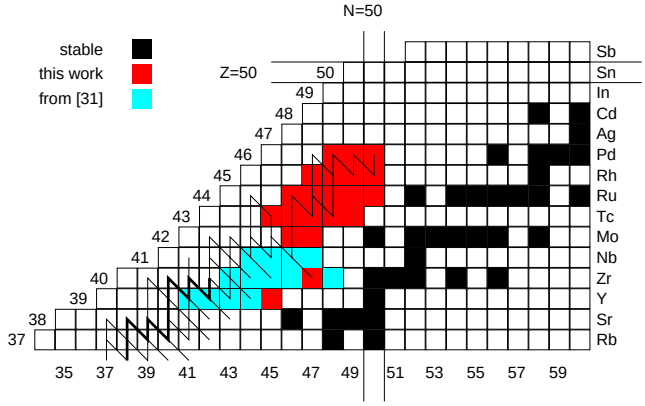

FIG. 12: The time-integrated reaction flow for the νp-process using the reaction rate set with the newly-determined mass values and the mass values from Ref. [31] substituted into the AME2003 mass data. The reaction flows shown are more than 10% (thick line) and 1–10% (thin line) of the reaction flow through the triple-α-reaction.

VIII. CONCLUSIONS

The mass values of 21 very neutron-deficient nuclides in the vicinity of the rp- and the νp-process pathways were determined by SHIPTRAP/GSI-Darmstadt and JYFLTRAP/Jyväskylä. The Penning trap data obtained at both facilities agree within their uncertainties and their weighted averages were given as the final results. For more than half of the data these are the first experimental determinations. A comparison with the data of the Atomic Mass Evaluation AME2003 and a detailed discussion of these and previous experimental results has been conducted for all nuclides. Most previous experimental determinations were stemming from β-endpoint measurements and large modifications of the mass surface are observed, in particular when approaching the $N = Z$ line, where experimental deviations along isobaric decay chains are accumulated and continued in the extrapolations. Now, the nuclear masses necessary for nuclear reaction-rate calculations are based to a large extent on experimental data. In addition, the new masses will improve the extrapolations for nuclei further away from stability.

The new data were used to perform calculations of the νp-process nucleosynthesis in order to check their impact on the reaction flow and the final abundances. To this end, reaction rates as well as Q values were re-calculated and have been compared with results employing the data from AME2003. The detailed flow patterns were established and compared. The new mass value for ^{88}Tc results in a proton-separation energy which is $\sim$ 1 MeV smaller than in the AME2003 systematics. Consequently,

the reaction flow around ^{88}Tc is strongly modified. However, the final abundances for the νp-process calculations are almost unchanged.

In order to improve the detailed modeling of the reaction pathways even further, a continuation of the measurement programme is desired as follows: among the nuclides already studied open questions of ambigous mass-to-state assignments should be revisited. These include the nuclides ^{84}Y, ^{85}Nb, ^{88}Tc, ^{90}Tc, and ^{92}Rh. Furthermore, specific nuclides with uncertain spin assignments and/or long-lived isomeric states should be extensively searched for to assess their possible influence in the rp- or νp-process [127]. Eventually new measurements should aim at a study further away from stability towards nuclei at the $N = Z$ line.

Acknowledgments

We acknowledge financial support by the EU within the networks NIPNET (contract HPRI-CT-2001-50034), Ion Catcher (contract HPRI-CT-2001-50022), EURONS (Joint Research Activities TRAPSPEC and DLEP), the Academy of Finland under the Finnish Centre of Excellence Programmes 2000-2005 (Project No. 44875, Nuclear and Condensed Matter Physics Programme) and 2006-2011 (Nuclear and Accelerator Based Physics Programme at JYFL), the Finnish-Russian Interacademy Agreement (Project # 8), the German Ministry for Education and Research (BMBF contracts: 06GF186I, 06GI185I, 06MZ215), and the Association of Helmholtz Research Centers (contracts: VH-NG-033, VH-NG-037). This work was supported in part by the Swiss NSF (grant 2000-105328). C.F. acknowledges support from an Enrico Fermi Fellowship.

[1] H. Stolzenberg *et al.*, Phys. Rev. Lett. **65** (1990) 3104.
[2] K. Blaum, Phys. Rep. **425** (2006) 1.
[3] L. Schweikhard and G. Bollen (Eds.), Special Issue on Ultra-accurate mass spectrometry and related topics, Int. J. Mass Spectrom. **251** (2006).
[4] K. Blaum *et al.*, Phys. Rev. Lett. **91** (2003) 260801.
[5] I.S. Towner and J.C. Hardy, Phys. Rev. C **77** (2008) 025501.
[6] T. Eronen *et al.*, Phys. Rev. Lett. **100** (2008) 132502.
[7] D.D. Warner, M.A. Bentley, and P. Van Isacker, Nature Physics **2** (2006) 311.
[8] H. Schatz *et al.*, Phys. Rep. **294** (1998) 167.
[9] B.A. Brown *et al.*, Phys. Rev. C **65** (2002) 045802.
[10] H. Schatz, Int. J. Mass Spectrom. **251** (2006) 293.
[11] C. Fröhlich *et al.*, Phys. Rev. Lett. **96** (2006) 142502.
[12] J. Pruet *et al.*, Astrophys. J. **644** (2006) 1028.
[13] S. Wanajo, Astrophys. J. **647** (2006) 1323.
[14] J. Äystö, Nucl. Phys. A **693** (2001) 477.
[15] J. Dilling *et al.*, Hyp. Interact. **127** (2000) 491.
[16] M. Block *et al.*, Eur. Phys. J. A. **25** S01 (2005) 49.
[17] G. Münzenberg *et al.*, Nucl. Instr. and Meth. Phys. Res. **161** (1979) 65.
[18] S. Hofmann and G. Münzenberg, Rev. Mod. Phys. **72** (2000) 733.
[19] J.B. Neumayr *et al.*, Nucl. Instr. Meth. B **244** (2006) 489.
[20] A. Nieminen *et al.*, Nucl. Instr. Meth. A **469** (2001) 244.
[21] F. Herfurth *et al.*, Nucl. Instr. Meth. A **469** (2001) 254.
[22] G. Sikler, Ph.D. thesis, University of Heidelberg (2003).
[23] V.S. Kolhinen, Ph.D. thesis, University of Jyväskylä (2003).
[24] V.S. Kolhinen *et al.*, Nucl. Instr. Meth. B **528** (2004) 776.
[25] G. Gabrielse, L. Haarsma, and S.L. Rolston, Int. J. Mass. Spectrom. Ion Process. **88** (1989) 319.
[26] H. Raimbault-Hartmann *et al.*, Nucl. Instr. Meth. B **126** (1997) 378.
[27] G. Savard *et al.*, Phys. Lett. A **158** (1991) 247.
[28] G. Gräff, H. Kalinowsky, and J. Traut, Z. Phys. A **297** (1980) 35.
[29] M. König *et al.*, Int. J. Mass. Spectrom. Ion Process. **142** (1995) 95.
[30] H. Schatz *et al.*, Phys. Rev. Lett. **86** (2001) 3471.
[31] A. Kankainen *et al.*, Eur. Phys. J. A **29** (2006) 271.
[32] A. Martín *et al.*, Eur. Phys. J. A **34** (2007) 341.
[33] V.-V. Elomaa *et al.*, to be submitted to Eur. Phys. J. A (2008).
[34] A. Kellerbauer *et al.*, Phys. Rev. C **76** (2007) 045504.
[35] T. Otto *et al.*, Nucl. Phys. A **567** (1994) 281.
[36] G. Sikler *et al.*, Nucl. Phys. A **763** (2005) 45.
[37] G. Audi, O. Bersillon, J. Blanchot, and A. H. Wapstra, Nucl. Phys. A **729** (2003) 3.
[38] Evaluated Nuclear Structure Data File, http://www.nndc.bnl.gov/ensdf/.
[39] S. Dean *et al.*, Eur. Phys. J. A **21** (2004) 243.
[40] E. Nolte and H. Hick, Z. Phys. A **305** (1982) 289.
[41] L.S. Brown and G. Gabrielse, Phys. Rev. A **25** (1982) 2423.
[42] L.S. Brown and G. Gabrielse, Rev. Mod. Phys. **58** (1986) 233.
[43] G. Bollen, R.B. Moore, G. Savard, and H. Stolzenberg, J. Appl. Phys. **68** (1990) 4355.
[44] M. Kretzschmar, Phys. Scr. **46** (1992) 544.
[45] M. Kretzschmar, Phys. Scr. **46** (1992) 555.
[46] K. Blaum *et al.*, Eur. Phys. J. A **15** (2002) 245.
[47] A. Kellerbauer *et al.*, Eur. Phys. J. D **22** (2003) 53.
[48] C. Rauth, Ph.D. Thesis, University of Heidelberg (2006).
[49] S. Rahaman *et al.*, Eur. Phys. J. A **34** (2007) 5.
[50] R. Birge, Phys. Rev. **40** (1932) 207.
[51] A. Chaudhuri *et al.*, Eur. Phys. J. D **45** (2007) 47.
[52] D. Tománek and M. A. Schluter, Phys. Rev. Lett. **67**

(1991) 2331.
[53] R. Ferrer, Ph.D. thesis, University of Mainz (2007).
[54] V.-V. Elomaa, Ph.D. thesis, University of Jyväskylä, in preparation.
[55] G. Audi, A.H. Wapstra, and C. Thibault, Nucl. Phys. A **729** (2003) 337.
[56] J.A. Clark *et al.*, Eur. Phys. J. A. **25** S01 (2005) 629.
[57] R. Iafigliola and J.K.P Lee, Phys. Rev. C **13** (1976) 2075.
[58] C.J. Lister *et al.*, Phys. Rev. C **24** (1981) 260.
[59] R.B. Firestone and V.S. Shirley, Table of Isotopes, 8th ed., Wiley (1996).
[60] J. Döring, A. Aprahamian, and M. Wiescher, J. Res. Natl. Inst. Stand. Technol. **105** (2000) 43.
[61] A.H. Wapstra, G. Audi, and C. Thibault, Nucl. Phys. A **729** (2003) 129.
[62] S. Kato *et al.*, Phys. Rev. C **41** (1990) 1276.
[63] R. Iafigliola, S.C. Gujrathi, B.L. Tracy, and J.K.P. Lee, Can. J. Phys. **52** (1974) 96.
[64] K. Oxorn and S.K. Mark, Z. Phys. A **303** (1981) 63.
[65] D. Rudolph *et al.*, Phys. Rev. C **47** (1993) 2574.
[66] R. Bass, Nuclear reactions with heavy ions, Text and monographs in Physics, Springer (1980).
[67] A. Kankainen *et al.*, submitted to Phys. Rev. Lett (2008), arXiv:0804.4743.
[68] D. Rudolph *et al.*, J. Phys. G **17** (1991) L113.
[69] M. Weiszflog *et al.*, Z. Phys. A **342** (1992) 257.
[70] A. Odahara *et al.*, Z. Phys. A **354** (1996) 231.
[71] M. Shibata *et al.*, J. Phys. Soc. Jpn. **65** (1996) 3172.
[72] D. Kast *et al.*, Z. Phys. A **356** (1997) 363.
[73] H. Herndl, B.A. Brown, Nucl. Phys. A **627** (1997) 35.
[74] I. Mukha *et al.*, Phys. Rev. Lett. **95** (2005) 022501.
[75] I. Mukha *et al.*, Nature **439** (2006) 298.
[76] E. Roeckl, Int. J. Mod. Phys. E **15** (2006) 368.
[77] O. Pechenaya *et al.*, Phys. Rev. C **76** (2007) 011304(R).
[78] J.B. Ball, Nucl. Phys. A **160** (1971) 225.
[79] K. Rykaczewski *et al.*, Z. Phys. A **322** (1985) 263.
[80] J. Ashkenazi *et al.*, Nucl. Phys. A **158** (1970) 146.
[81] R.C. Pardo *et al.*, Phys. Rev. C **18** (1978) 1249.
[82] Yu.A. Litvinov *et al.*, Nucl. Phys. A **756** (2005) 3.
[83] R.C. Pardo *et al.*, Phys. Rev. C **21** (1980) 462.
[84] K. Heiguchi *et al.*, Z. Phys. A **338** (1991) 7.
[85] D. Rudolph *et al.*, Nucl. Phys. A **587** (1995) 181.
[86] E. Hagberg *et al.*, Nucl. Phys. A **395** (1983) 152.
[87] J. Äystö *et al.*, Nucl. Phys. A **404** (1983) 1.
[88] C. Weiffenbach, S.C. Gujrathi, and J.K.P. Lee, Can. J. Phys. **53** (1975) 101.
[89] E. Nolte, G. Korschinek and U. Heim, Z. Phys. A **298** (1980) 191.
[90] R.A. Pinston, E. Monnand, and A. Moussa, Jour. de Phys. **29** (1968) 257.
[91] C.F. Moore *et al.*, Phys. Rev. **141** (1966) 1166.
[92] S.I. Hayakawa *et al.*, Nucl. Phys. A **199** (1973) 560.
[93] K. Oxorn, B. Singh, and S.K. Mark, Z. Phys. A **294** (1980) 389.
[94] E. Roeckl *et al.*, Nucl. Instr. Meth. A **204** (2003) 53.
[95] W. Kurcewicz *et al.*, Z. Phys. A **308** (1982) 21.
[96] W.J. Mills *et al.*, Phys. Rev. C **75** (2007) 047302.
[97] L. Batist *et al.*, Eur. Phys. J. A **29** (2006) 175.
[98] PACE4, fusion-evaporation code, http://www.nscl.msu.edu/lise (2005).
[99] E. Nolte and H. Hick, Phys. Lett. B **97** (1980) 55 and [40].
[100] K. Ogawa, Phys. Rev. C **28** (1983) 958.
[101] J. Döring *et al.*, GSI Annual Report 2003.
[102] S.E. Arnell *et al.*, Phys. Rev. C **49** (1994) 51.
[103] K. Schmidt *et al.*, Nucl. Phys. A **624** (1997) 185.
[104] N. Mărginean, Eur. Phys. J. A **20** (2004) 123.
[105] T. Kuroyanagi *et al.*, Nucl. Phys. A **484** (1988) 264.
[106] J. Van Roosbroeck *et al.*, Phys. Rev. Lett. **92** (2004) 112501.
[107] K. Blaum *et al.*, Europhys. Lett. **67** (2004) 586.
[108] S. Rinta-Antila *et al.*, Eur. Phys. J. A **31** (2007) 1.
[109] J. Hakala *et al.*, Phys. Rev. Lett **101** (2008) 052502.
[110] S. Rahaman *et al.*, Eur. Phys. J. A **32** (2007) 87.
[111] P. Delahaye *et al.*, Phys. Rev. C **74** (2006) 034331.
[112] G. Lhersonneau *et al.*, Phys. Rev. C **49** (1994) 1379.
[113] P. Campbell *et al.*, Phys. Rev. Lett. **89** (2002) 082501.
[114] B. Cheal *et al.*, Phys. Lett. B **645** (2007) 133.
[115] R.K. Wallace and S.E. Woosley, Astrophys. J. Suppl. **45** (1981) 389.
[116] R. Buras *et al.*, Astron. and Astrophys. **447** (2006) 1049.
[117] M. Liebendörfer *et al.*, Phys. Rev. D **63** (2001) 103004.
[118] T.A. Thompson, E. Quataert, and A. Burrows, Astrophys. J. **620** (2005) 861.
[119] R. Surman *et al.*, American Institute of Physics Conference Series **990** (2008) 297.
[120] H.-T. Janka, R. Buras, and M. Rampp, Nucl. Phys. A **718** (2003) 269.
[121] J.L. Fisker, R.D. Hoffman, and J. Pruet (2007), astroph/0711.1502.
[122] T. Rauscher, in preparation.
[123] T. Rauscher and F.-K. Thielemann, in "Stellar Evolution, Stellar Explosions, and Galactic Chemical Evolution", ed. A. Mezzacappa (IOP, Bristol 1998), p. 519.
[124] T. Rauscher and F.-K. Thielemann, At. Data Nucl. Data Tables **75** (2000) 1.
[125] NuDat 2.4, National Nuclear Data Center, http://www.nndc.bnl.gov/nudat2/.
[126] K. Lodders, Astrophys. J. **591** (2003) 1220.
[127] Yu.N. Novikov *et al.*, Eur. Phys. J. A **11** (2001) 257.

[128] This quantity depends on the cyclotron frequency ν_c and the duration T_{RF} of the measurement.
[129] The estimated values of the molecular binding energy/atom of the carbon clusters varies from 3.1 eV in $^{12}C_2$ to 7.0 eV in $^{12}C_{60}$ [52], therefore it is negligible at the present uncertainty level for mass measurements at both facilities.
[130] ^{58}Ni : 68.0769(89)%, ^{60}Ni : 26.2231(77)%, ^{61}Ni : 1.1399(6)%, ^{62}Ni : 3.6345(17)%, ^{64}Ni : 0.9256(9)%, http://www.webelements.com.
[131] Note that a possible lower value in the excitation energy of ^{90}Tc^m will affect this estimate.
[132] A correction due to an unknown contribution of isomeric states has been applied for the data from Ref. [31].
[133] Number of successive links indicating the distance to the primary data set in the atomic mass evaluation.